Black Death - Blue Skies - White Clouds

Water Vapour Uptake of Particles Produced from Traffic Exhaust and their Effect on Climate

Wittbom, Cerina

2017

Document Version:
Other version

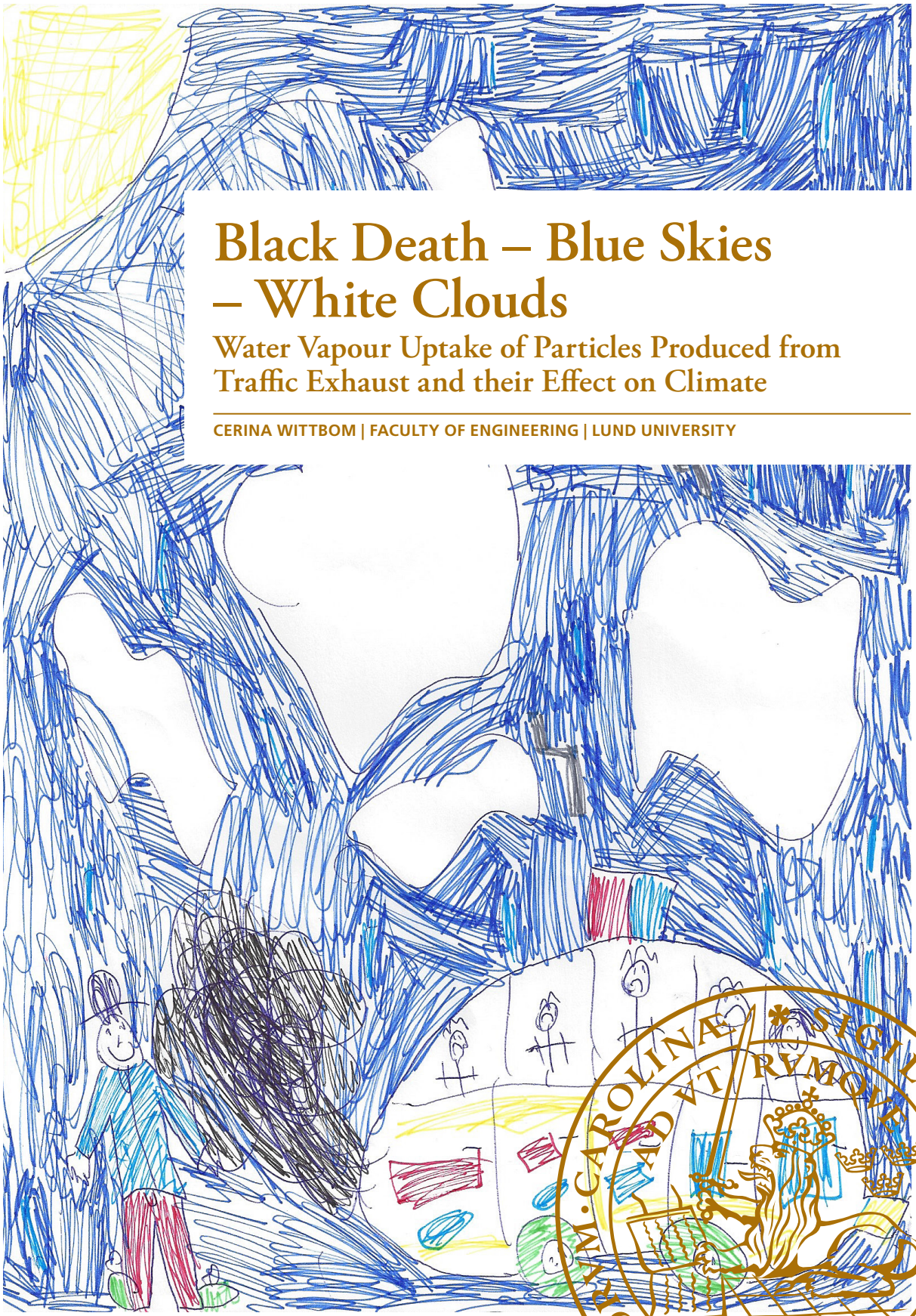

Black Death – Blue Skies – White Clouds

Water Vapour Uptake of Particles Produced from Traffic Exhaust and their Effect on Climate

CERINA WITTBOM | FACULTY OF ENGINEERING | LUND UNIVERSITY

Printed by Media-Tryck, Lund 2017 NORDIC ECOLABEL. 3041 0903

Author's Comment

We can no longer produce and release vast amounts of combustion emissions, and close our eyes to the effects they have on both the climate and human health. We can no longer blame "someone else" for not reducing "their" emissions. Anthropogenic emissions are a global issue. New, cleaner technology is of course very important, but what is really needed is a change in our behaviour and the way we think to deal with the challenges we face in reducing emissions. Combustion emissions contribute to a large extent to outdoor air pollution. It has been estimated that outdoor air pollution causes about 4 million premature death every year. This number may increase drastically if we allow the rate of climate change to continue as it is today. Sceptics may say that we don't know what the future might bring, but I believe we cannot just sit and wait to see whether life on Earth as we know it today, will be destroyed by our own actions.

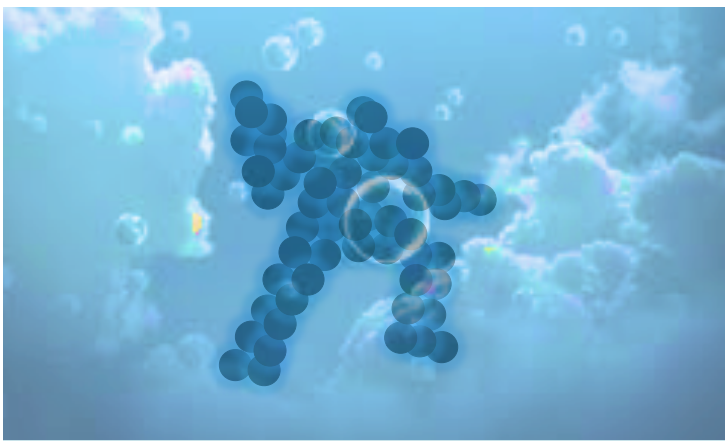

LUND UNIVERSITY

Lund University
Faculty of Engineering
Division of Nuclear Physics
ISBN 978-91-7753-267-5

Black Death

Blue Skies

White Clouds

Black Death – Blue Skies

– White Clouds

Water Vapour Uptake of Particles Produced from Traffic Exhaust and their Effect on Climate

Cerina Wittbom

LUND
UNIVERSITY

DOCTORAL DISSERTATION
which by due permission of the Faculty of Engineering, Lund University, Sweden, will be defended on 19 May 2017 at 9.00 a.m. in the Rydberg Lecture Hall, at the Department of Physics, Sölvegatan 14A, Lund.

Faculty opponent
Dr Heike Wex

Department of Experimental Aerosol and Cloud Microphysics, Leibniz Institute for Tropospheric Research

Organization	Document name
LUND UNIVERSITY	DOCTORAL DISSERTATION
Division of Nuclear Physics Box 118, SE-22100, Lund	Date of issue
Author(s) Cerina Wittbom	Sponsoring organization

Title and subtitle

Black Death – Blue Skies – White Clouds

Water Vapour Uptake of Particles Produced from Traffic exhaust and their Effect on Climate

Abstract

Aerosol particles are everywhere in the air around us, regardless of whether you are in a busy city or in the serene Arctic. Airborne particles can be produced naturally or anthropogenically, and their properties changes during the time they spend in the atmosphere. Their sizes range from about 1 nm to 100 µm, and affect us in two ways; firstly, our health by deposition in the respiratory tract, and secondly via pertubation of the climate. The Earth's climate is affected by the radiation balance, which is in turn affected by the presence of particles and the formation of cloud droplets. Cloud droplets form on pre-existing particles by condensation of water vapour. These particles, which act as seeds for the condensation of water, are called cloud condensation nuclei (CCN).

The ability of particles to take up water vapour depends on their chemical and physical properties, and is described by particle hygroscopicity. The theoretical framework used in this work to calculate particle hygroscopicity was first introduced by Köhler in 1936, and has since then been developed to account for non-ideal conditions.

Particle hygroscopicity of fresh and aged traffic exhaust was investigated in laboratory measurements. The complete transformation of soot particles, from fresh emissions of hydrophobic, aspherical soot agglomerates to compacted soot particles coated with secondary organic aerosol (SOA), which are able to act as CCN, was captured for the first time. The SOA produced from traffic emissions showed differences in water vapour uptake, when measured in the subsaturated compared to supersaturated regimes. Theoretical analysis using modified Köhler theory, indicated that these measured differences could be explained by limitation of the solubility of the SOA that was condensed on the seed particles.

Ambient measurements of particle hygroscopicity associated with traffic emissions were performed in urban and rural environments. The urban aerosol showed a clear diurnal variation as well as a dependence on air mass origin. The fraction of particles with low hygroscopicity and the fraction of fresh soot (from traffic) showed good agreement during the daytime. However, during the night-time the fraction of agglomerated soot decreased, probably as a result of soot emissions from further away having undergone ageing, and hence restructured to more dense particles, while the hygroscopicity was not notably improved. Furthermore, observations made by following air masses from the urban to the rural environments showed that soot particle restructuring and changes in their properties may occur much faster than previously thought (within 5 hours), due to particulate nitrate formation coupled to water vapour uptake.

Finally, the impact of traffic exhausts on climate was synthetized by combining the results in this thesis with those from the literature. Soot particles lead mainly to global warming. Traffic emissions can also reduce visibility, as the ability to absorb and scatter light may increase with ageing and water vapour uptake. However, with further ageing and increased hygroscopicity, the particles produced by traffic can act as cloud condensation nuclei, thus contributing to cooling. The increased hygroscopicity (due to condensation of organic and inorganic material) will affect the atmospheric lifetime of the soot particles, which also influence climate change.

Key words: Aerosol particles, cloud condensation nuclei, hygroscopicity, climate, organic particles, soot

Classification system and/or index terms (if any)

Supplementary bibliographical information		Language English
ISSN and key title		ISBN 978-91-7753-267-5 (print) 978-91-7753-268-2 (pdf)
Recipient's notes	Number of pages 194	Price
	Security classification	

Signature 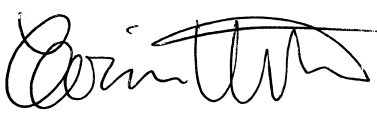 Date 2017-04-11

Black Death – Blue Skies – White Clouds

Water Vapour Uptake of Particles Produced from Traffic Exhaust and their Effect on Climate

Cerina Wittbom

LUND
UNIVERSITY

Cover illustration by Hilda Wittbom

Department of Physics |Faculty of Engineering | Lund University

ISRN LUTFD2/(TFKF-1049)/1 - 68 (2017)
ISBN 978-91-7753-267-5 (print)
ISBN 978-91-7753-268-2 (pdf)

Printed in Sweden by Media-Tryck, Lund University
Lund 2017

Till Andreas, Hilda, Erik och Kajsastina

Papers Included in this Doctoral Thesis

This thesis is based on the following papers or manuscripts, which will be referred to in the text by their Roman numerals. The papers or manuscripts are appended at the end of the thesis.

I **Wittbom, C.**, Eriksson, A. C., Rissler, J., Carlsson, J. E., Roldin, P., Nordin, E. Z., Nilsson, P. T., Swietlicki, E., Pagels, J. H. and Svenningsson, B.

Cloud droplet activity changes of soot aerosol upon smog chamber ageing.

Atmospheric Chemistry and Physics 14, no. 18 (2014): 9831-9854.

II **Wittbom, C.**, Eriksson, A., Rissler, J., Roldin, P., Nordin, E.Z., Sjogren, S., Nilsson, P.T., Swietlicki, E., Pagels, J., and Svenningsson, B.

Effect of solubility limitation on hygroscopic growth and CCN activation of SOA particles produced from traffic exhausts.

To be submitted.

III **Wittbom, C.**, Sjogren, S., Eriksson, A.C., Sporre, M., Rissler, J., Martinsson, J., Swietlicki, E., and Svenningsson, B.

Hygroscopic properties of aerosol particles in a near-traffic urban environment.

To be submitted

IV Eriksson, A. C., **Wittbom, C.**, Roldin, P., Sporre, M., Öström, E., Nilsson, P., Martinsson, J., Rissler, J., Nordin, E. Z., Svenningsson, B., Pagels, J., and Swietlicki, E.

Diesel soot aging in urban plumes within hours under cold, dark and humid conditions.

Submitted to Nature Communication.

V **Wittbom, C.**, and Svenningsson, B.

Traffic exhaust, hygroscopicity and climate.

To be submitted.

The author's contribution to the papers

I & II	I participated in planning and took part in part of the experiments. I participated in implementing and evaluating the scanning flow CCN analysis procedure. I analysed the particle water vapour uptake, and participated in the analysis of the mass-mobility relationship and the chemical composition. I wrote the paper with input from the other authors. The ADCHAM modelling was performed by one of the co-authors. (These two papers are based on the same experimental campaign.)
III	I participated in planning the measurement campaign. I analysed the particle water vapour uptake in the supersaturated regime. I took part in the analysis and discussions of the water vapour uptake in the subsaturated regime, the chemical composition, the size distribution, and meteorological data. I wrote the paper together with the other authors.
IV	I performed the analysis of the particle water vapour uptake. I took part in the analysis of the chemical composition and contributed to writing the paper, especially the part concerning particle hygroscopicity and the restructuring of soot particles.
V	I wrote the paper with input from the other author. Paper V is a synthesis of Papers I-IV, which places the experimental work and results from the literature in perspective.

Related publications

Peer-reviewed papers

Nordin, E. Z., Eriksson, A. C., Roldin, P., Nilsson, P. T., Carlsson, J. E., Kajos, M. K., Hellén, H., **Wittbom, C.**, Rissler, J., Löndahl, J., Swietlicki, E., Svenningsson, B., Bohgard, M., Kulmala, M., Hallquist, M., and Pagels, J. H.

Secondary organic aerosol formation from gasoline passenger vehicle emissions investigated in a smog chamber

Atmos. Chem. Phys. 13, 6101–6116.

Paramonov, M., Kerminen, V.-M., Gysel, M., Aalto, P.P., Andreae, M.O., Asmi, E., Baltensperger, U., Bougiatioti, A., Brus, D., Frank, G.P., Pöschl, U., Roberts, G.C., Rose, D., Svenningsson, B., Swietlicki, E., Weingartner, E., Whitehead, J., Wiedensohler, A., **Wittbom, C.**, Sierau, B.

A synthesis of cloud condensation nuclei counter (CCNC) measurements within the EUCAARI network

Atmos. Chem. Phys. 21:12211-12229.

Schmale, J., Henning, S., Henzing, B., Keskinen, H., Sellegri, K., Ovadnevaite, J., Bougiatioti, A., Kalivitis, N., Stavroulas, I., Jefferson, A., Park, M., Schlag, P., Kristensson, A., Iwamoto, Y., Pringle, K., Reddington, C., Aalto, P., Äijälä, M., Baltensperger, U., Bialek, J., Birmili, W., Bukowiecki, N., Ehn, M., Fjæraa, A. M., Fiebig, M., Frank, G., Fröhlich, R., Frumau, A., Furuya, M., Hammer, E., Heikkinen, L., Herrmann, E., Holzinger, R., Hyono, H., Kanakidou, M., Kiendler-Scharr, A., Kinouchi, K., Kos, G., Kulmala, M., Mihalopoulos, N., Motos, G., Nenes, A., O'Dowd, C., Paramonov, M., Petäjä, T., Picard, D., Poulain, L., Prévôt, A. S. H., Slowik, J., Sonntag, A., Swietlicki, E., Svenningsson, B., Tsurumaru, H., Wiedensohler, A., **Wittbom, C**., Ogren, J. A., Matsuki, A., Yum, S. S., Myhre, C. L., Carslaw, K., Stratmann, F., and Gysel, M.

Collocated observations of cloud condensation nuclei, particle size distributions, and chemical composition

Scientific Data, 4, 170003, 10.1038/sdata.2017.3

Conference abstracts as lead author

Wittbom, C., Svenningsson, B., Rissler, J., Fors, E., Swietlicki, E., Nordin, E., Eriksson, A., Nilsson, P., and Pagels, J. *Hygroscopic and cloud-activation properties of aged exhaust aerosols*. International Aerosol Conference, 2010.

Wittbom, C., Svenningsson, B., Rissler, J., Swietlicki, E., Nordin, E., Eriksson, A., Nilsson, P., and Pagels, J. *WP1: Altered hygroscopic and cloud-activation properties during the ageing process of exhaust aerosol*. Lund University Centre for Studies of Carbon Cycle and Climate Interactions Annual Meeting, 2012.

Wittbom, C., Svenningsson, B., Rissler, J., Eriksson, A., Swietlicki, E., Nordin, E., Nilsson, P., and Pagels, J. *Changes in hygroscopicity and cloud-activation of diesel exhaust aerosols upon ageing*. European Aerosol Conference, 2012.

Wittbom, C., Svenningsson, B., Rissler, J., Eriksson, A., Swietlicki, E., Nordin, E. Z., Nilsson, P. T., and Pagels, J. *Changes in Hygroscopicity and Cloud-Activation of Diesel Soot upon Ageing*. Nordic Society for Aerosol Research Symposium, 2012.

Wittbom, C., Pagels, J., Rissler, J., Eriksson, A. C., Swietlicki, E., Carlsson, J. E., Nordin, E. Z., Roldin, P., Nilsson, P. T., and Svenningsson, B. *Ageing soot as cloud condensation nuclei*. Cryosphere-Atmosphere Interactions in a Changing Arctic Climate, 2013.

Wittbom, C., Svenningsson, B., Sjogren, S., and Swietlicki, E. *Evaluation and development of Scanning Flow CCN Analysis*. European Aerosol Conference, 2013.

Wittbom, C., Pagels, J., Rissler, J., Eriksson, A. C., Carlsson, J. E., Roldin, P., Nordin, E. Z., Nilsson, P. T., Swietlicki, E., and Svenningsson, B. *Cloud droplet activity changes of soot aerosol upon smog chamber ageing*. Lund University Centre for Studies of Carbon Cycle and Climate Interactions, Annual Report, 2013.

Wittbom, C., Pagels, J., Rissler, J., Eriksson, A., Nordin, E.Z., Nilsson, P., Swietlicki, E., and Svenningsson, B. *Hygroscopicity of photochemical processed particles from three different sources*. Lund University Centre for Studies of Carbon Cycle and Climate Interactions, Annual Report, 2015.

Wittbom, C., Poulsen, M.B., Pei, X.Y., Pathak, R.K., Hallquist, M., Eriksson, A., Nordin, E.Z., Ahlberg, E., Pagels, J., Rissler, J., Swietlicki, E., and Svenningsson, B. *Cloud droplet activity measurements of coated soot particles*. Nordic Society for Aerosol Research Symposium, 2015.

Wittbom, C., Sjogren, S., Rissler, J., Eriksson, A., Roldin, P., Nordin, E., Nilsson, P.T., Swietlicki, E., Pagels, J., and Svenningsson, B. *Combining CCN Activation and Hygroscopic Growth of Anthropogenic SOA Particles*. Cryosphere-Atmosphere Interactions in a Changing Arctic Climate, 2016.

Wittbom, C., Sjogren, S., Rissler, J., Eriksson, A., Roldin, P., Nordin, E., Nilsson, P.T., Swietlicki, E., Pagels, J., and Svenningsson, B. *Combining CCN Activation and Hygroscopic Growth of Anthropogenic SOA Particles*. 13th Informal Conference on Atmospheric and Molecular Science, 2016.

Populärvetenskaplig sammanfattning

Jorden med sin respektabla ålder av mellan 4,5 och 4,6 miljarder år har varit med om en hel del klimatförändringar. För cirka 2000 miljoner år sedan möjliggjordes liv på land genom att encelliga alger i havet genom fotosyntes producerade syrgas. Utan en skyddande atmosfär kring jorden hade det inte varit möjligt för livet på jorden, så som det ser ut idag. Atmosfären, med en sammansättning liknande den vi har idag, tror man bildades för ca 600 miljoner år sedan. För att moln ska bildas i vår atmosfär krävs partiklar i luften som kan agera som kärnor för vattenånga att kondensera på. Utan partiklarna hade det krävts en betydligt högre luftfuktighet för att skapa molndroppar. Moln och dimma har många funktioner i jordens hydrologiska cykel. Till exempel sker förflyttning av vatten mellan olika reservoarer genom molnbildning och nederbörd, kemisk omvandling av olika ämnen, reglering av strålningsbalansen och så vidare. Partiklarna, vilka en och en är så små att vi inte kan se dem med blotta ögat, fyller en stor funktion på en global arena och påverkar oss dubbelt upp genom att påverka såväl vår hälsa som vårt klimat. Partiklar och gaser produceras naturligt i atmosfären i stora mängder. Sedan 1850-talet när människan började producera partiklar och gaser från förbränning i stor skala (fossila bränslen) har dock jordens klimat förändrats i en större utsträckning än tidigare – vi går mot ett varmare klimat. Vår jord, å ena sidan, bryr sig inte nämnvärt över våra utsläpp och det medföljande varmare klimatet – jorden har klarat både varmare och kallare perioder galant tidigare. För människans del, å andra sidan, får utsläppen av förbränningsaerosol (som innehåller såväl koldioxid som partiklar) katastrofala följder, både klimatmässigt och hälsomässigt.

Denna avhandling belyser interaktionen mellan vattenånga och partiklar producerade från trafikavgaser, samt hur interaktionen med vattenånga förändras när partiklarna åldras under sin tid i atmosfären. Genom att undersöka bilavgaser i laboratorium kan vi konstatera att färska sotpartiklar inte tar upp vatten vid den luftfuktighet som råder i atmosfären. När sotpartiklarna åldras kondenserar gaser, av vilka en del har sitt ursprung i bilavgaserna, på partiklarna. Detta förändrar deras struktur till en mer kompakt form och underlättar vattenupptaget från deras omgivning. Partiklarnas vattenupptag kan modelleras, men man måste beakta att de organiska ämnen som produceras från bilavgaserna har en begränsad löslighet – vilket vi visar i denna avhandling – och inte tar upp vatten i samma utsträckning som inorganiska ämnen. Från mätningar utförda i Köpenhamn kan man konstatera att en stor andel av partiklarna under dagtid (antalsmässigt) består av färska, lokalt producerade sotpartiklar, främst från trafikavgaser, som tar upp en väldigt begränsad mängd vatten. Nattetid, visar mätningarna att många av partiklarna fortfarande har ett begränsat vattenupptag, men är mer kompakta i sin struktur.

Dessa observationer stämmer väl överens med laboratoriemätningar, där kompakteringen sker långt innan en mätbar skillnad i vattenupptag är synlig, vid låg luftfuktighet. Vid hög luftfuktighet (så som i moln) syns ett ökat vattenupptag betydligt tidigare. De aerosolpartiklar som transporterats långväga har hunnit åldras mer och visar därför ett högre vattenupptag än de som produceras lokalt. Dock kan åldring av sot gå fort i atmosfären, om inorganiska salter kondenserar på partiklarna. Partiklars vattenupptag har betydelse för såväl sikten som molndroppsbildning och påverkar därigenom klimatet. Sotpartiklar och andra partiklar producerade från trafikavgaser kan påverka oss både där de produceras lokalt och globalt, genom långväga transporter i atmosfären. Vattenupptaget har även betydelse för deponeringen av partiklar i våra lungor (där luftfuktigheten är hög). Med andra ord påverkas vi av partiklarnas förmåga att ta upp vatten på två sätt: direkt genom deponering i våra lungor och indirekt genom förändringar av klimatet.

Klimatforskning utgör ett jättepussel med oändligt många bitar. Denna avhandling utgör en av alla dessa bitar, som förhoppningsvis bidrar till att vi i framtiden (innan det är för sent) kan lägga det stora pusslet.

Nomenclature

a_w	Water activity
ADCHAM	Aerosol Dynamics, gas- and particle- phase chemistry model for laboratory CHAMber studies
AMS	Aerosol mass spectrometer
AS	Ammonium sulphate
BC	Black carbon
C_c	Cunningham slip correction factor
CCN	Cloud condensation nuclei
CCNC	Cloud condensation nuclei counter
CFSTGC	Continuous-flow streamwise thermal-gradient counter
CPC	Condensational particle counter
$C_{sat,s}$	Solubility (mass per unit volume) of compound *s* in water
D	Diameter of the spherical aqueous solution droplet
DMA-APM	Differential mobility analyser-aerosol particle mass analyzer
d_s	Diameter of the dry particle
d_{va}	Vacuum aerodynamic diameter
d_{ve}	Volume equivalent diameter
d_z	Mobility diameter
$d(RH)$	The mean diameter of the conditioned aerosol size distribution
ERFaci	Effective radiative forcing from aerosol-cloud interactions
gf	Hygroscopic growth factor
HR-ToF-AMS	High-resolution time of flight mass spectrometer
H-TDMA	Hygroscopic tandem differential mobility analyser
i	van't Hoff factor, a measure of the effects of ion interactions and dissociation on water activity
IPCC	Intergovernmental Panel on Climate Change
IVOC	Intermediate volatility organic compounds
i_s	van't Hoff factor for a specific component *s*
Ke	Kelvin effect
M_s	Molecular mass for a specific component *s*
M_w	Molecular mass for water
$NF_{gf<1.25}$	Number fraction of less-hygroscopic particles (with a gf<1.25)
NF_{soot}	Number fraction of soot in relation to dense particles
n_s	Number of moles of substance in the solution
n_{sum}	Sum of the moles of the different contributing components in the particles
n_w	Number of moles of water in the solution
OPC	Optical particle counter
P	Pressure

p	Actual partial pressure
p_0	Equilibrium pressure over a flat surface of pure water
Q	Flow rate
Q_{50}	Critical flow rate
R	Universal gas constant
RH	Relative humidity
RFari	Radiative forcing from aerosol-radiation interactions
s	Saturation ratio
s_c	Critical supersaturation
SFCA	Scanning flow CCN analysis
SMPS	Scanning mobility particle sizer
SOA	Secondary organic aerosol
SP-AMS	Soot particle aerosol mass spectrometer
T	Absolute temperature
TEM	Transmission electron microscopy
VOC	Volatile organic compound
ZSR	Zdanovskii, Stokes, and Robinsson mixing rule
ΔT	Streamwise temperature gradient
β_s	Mass fraction of component s in the initial dry particle
ε_s	Volume fraction of a specific component s in the dry particle
κ	Hygroscopicity parameter describing the number of ions or non-dissociating molecules per unit volume of the dry particle
κ_{gf}	Value of the hygroscopicity parameter derived from the measured growth factor
κ_{chem}	Value of the hygroscopicity parameter calculated from the chemical composition
κ_{sc}	Value of the hygroscopicity parameter derived from the measured critical supersaturation
v	Dissociation number
ρ_0	Density of the dry particle (Eq.6) assuming volume additivity
ρ_p	Particle density (including preserved internal void spaces as a phase with zero density)
ρ_s	Density of a specific component s
ρ_{st}	Standard density (1000 kg m^{-3})
ρ_w	Density of water
$\sigma_{s/a}$	Surface tension of the solution droplet
χ	Dynamic shape factor (all flow regimes)
χ_t	Dynamic shape factor (transition regime)
χ_v	Dynamic shape factor (vacuum or free molecular regime)

Contents

Aims of this Research

The overall aim of the work presented in this thesis is to study particles produced from traffic exhaust and their effect on climate. Our climate is affected by the radiation balance, which is in turn affected by the formation of cloud droplets. Cloud droplets are formed by the condensation of water vapour on ambient aerosol particles. The ability to take up water varies between particles depending on their chemical and physical properties. More specifically, the focus of this work was on traffic exhausts and their effects on water vapour uptake and cloud droplet activation.

Both laboratory and atmospheric measurements were performed to investigate how the anthropogenic secondary organic aerosol (SOA), produced from the traffic exhausts, influences the water vapour uptake. The changes in water vapour uptake of ageing soot particles were also investigated. The hygroscopicity of the soot particles is related to the secondary material condensing on the particle during atmospheric ageing. The increased water uptake by the soot particles facilitates the ability of the particles to form cloud droplets.

Laboratory and atmospheric (urban and rural) measurements were performed in both the subsaturated and supersaturated regimes in order to improve the theoretical framework for the predictions of the critical supersaturation for particles with complex chemical compositions.

Some parts of the text in this thesis have been revised from the author's Licentiate Dissertation, entitled "Cloud Droplet Forming Potential of Ageing Soot and Surfactant Particles" (Wittbom, 2014).

Background

Climate

The Earth's climate system includes the atmosphere, land, oceans, snow, ice, and all living things. Our climate is changing at a faster rate than ever before (IPCC, 2013), as evidenced by the increases in greenhouse gases, rise in global temperature, the diminishing snow and ice covers, and the rise in sea level. The natural atmospheric greenhouse is perturbed by human activities, such as the burning of fossil fuels, which increases the concentration of carbon dioxide (CO_2), the most important and long-lived greenhouse gas. However, anthropogenic emissions of aerosol particles can counter-act and cool the planet, masking the warming effect of greenhouse gases.

Aerosol particles can reflect or absorb light, both of which affect the radiation balance, and thus the climate. Soot particles, for example, absorb light leading to warming, while sulphate particles scatter light leading to cooling. The direct effects of particles on radiation are well understood and are said to have a high scientific understanding. It has been predicted that the total effective radiative forcing due to aerosols will lead to cooling of the planet (IPCC, 2013). Aerosol particles can also influence the Earth's climate and its hydrological cycle by acting as seeds for the condensation of water vapour, i.e. they can act as cloud condensation nuclei (CCN). As particles become cloud droplets, their properties change, as does their effect on the climate. This effect, which is less well understood, is referred to as the effective radiative forcing from aerosol-cloud interactions (IPCC, 2013), including, for instance, an increase in cloud albedo (reflectivity) due to addition of cloud nuclei by pollution (Twomey, 1974), increased cloud lifetime (Albrecht, 1989) and cloud thickness (Pincus and Baker, 1994), and daytime clearing of clouds due to soot aerosol abundance (Ackerman et al., 2000). The properties of particles change during the time spent in the atmosphere (residence time). For example, fresh soot agglomerates have a very low hygroscopicity whereas aged, more spherical soot particles are more hygroscopic, and can contribute to the population of CCN (see e.g. Tritscher et al., 2011; Weingartner et al., 1997).

Aerosols, health and climate

Aerosols can affect humans in two ways. Health can be affected directly, by the inhalation of aerosol particles, which are then deposited in the respiratory. It has been estimated by the WHO (2014) that around 6.5 million premature deaths were caused by poor indoor and outdoor air quality in 2012, i.e. one in eight of total global deaths. This high estimate makes air pollution the world's largest single environmental health risk. The most prominent causes of deaths due to air pollution are cardiovascular diseases, such as ischaemic heart disease and stroke, chronic obstructive pulmonary disease, lung cancer, and acute lower respiratory infections in children. Our health can also be affected indirectly by changes in the climate, due to pollution, for example, increasing temperatures and extreme weather events. The WHO (2016) has estimated that climate change will cause an additional 250 000 deaths every year, between 2030 and 2050, due to heat exposure of the elderly, diarrhoea, malaria and childhood undernutrition. In addition, the UNHCR (2015, and references therein) has reported that an annual average of about 26 million people migrate due to weather-related hazards associated with climate change, and it has been projected that the displacement of people will increase in the future (IPCC, 2014). However, estimates of health effects due to climate change are very uncertain.

The effects of aerosol particles on health and the climate are interlinked, and it is highly debated how to form legislation. Although reducing air pollution would lead to a decrease in the numbers of deaths, particles can also cool the planet, and reducing particle concentrations may thus lead to an increase greenhouse warming, leading to more deaths. One pollutant that can be reduced is soot (or black carbon, BC), which could be beneficial to both human health and the climate. It has been estimated that BC is the strongest anthropogenic climate-forcing agent in the present-day atmosphere, after CO_2 (Bond et al., 2013), and four major cities recently moved to ban diesel vehicles by 2025 (McGrath, 2016). Emissions of soot are hazardous to human health (e.g.Novakov and Rosen, 2013; Vermeulen et al., 2014; WHO, 2012). In addition, freshly emitted soot particles absorb light, leading to warming. The hygroscopicity of soot particles is enhanced during photochemical processing in the atmosphere (Tritscher et al., 2011). As the hygroscopicity increases, the deposition pattern of particles in the respiratory system also changes (Londahl et al., 2009; Rissler et al., 2012) as does the effect that soot particles have on the Earth's hydrological cycle, and thus the climate (Bond et al., 2013).

Aerosol particles and cloud droplets

An aerosol is a gaseous medium in which solid or liquid particles are suspended (Hinds, 2012). Hence, the air around us is an aerosol and with every breath we take, we inhale millions of aerosol particles. The particles present in the atmosphere can be of many kinds, and vary greatly in their physical and chemical properties, concentration, and residence time. The effect these particles have on the surrounding environment change as their properties vary. Therefore, in order to be able to describe the whole picture, for example, how the particles scatter or absorb light in the atmosphere, or predict how particles become deposited in the human respiratory tract, it is important to know the particle concentration (in terms of number, mass or volume), their properties and their size distribution.

Particles can be produced from both natural and anthropogenic sources. Examples of different particles are soil particles, sea spray particles, volcanic particles, bacteria and other bioaerosol, combustion particles, nano-engineered particles, photochemically formed particles, and cloud droplets or ice particles (Andreae and Rosenfeld, 2008). Aerosol particle sizes range from a few nm in diameter up to ~100 μm (this size range can be understood by comparing a hot-air balloon to the Earth). Particles with a diameter greater than ~100 μm have too high a sedimentation rate to remain in suspension. In urban areas, for example, beside a busy road, the average number concentration of particles can be as high as 160 000 cm^{-3} (e.g. Shi et al., 1999; Weber et al., 2006; Wehner and Wiedensohler, 2003), whereas, the number concentration in remote locations such as the Arctic can be as low as 30 cm^{-3} (sometimes lower) (Covert et al., 1996). The residence time of a particle in the atmosphere can range from a few seconds, for freshly produced particles, to more than a year for particles that have reached the stratosphere. A primary aerosol particle is a particle introduced directly into the atmosphere, while a secondary aerosol particle is formed via gas-to-particle conversion processes in the atmosphere. In a heterogeneous aerosol, the particles differ in chemical composition, while in a homogeneous aerosol all the particles are chemically identical. Atmospheric aerosols are commonly composed of particles with a wide size range, and are referred to as polydisperse. Monodisperse aerosols, with particles of the same size, are often produced in the laboratory for tests.

Aerosol particles are necessary for cloud droplets to form in the atmosphere. Without aerosol particles, a relative humidity (RH) of 400% would be required for pure water droplets to form. As mentioned previously, particles that act as seeds for cloud droplets are called cloud condensation nuclei (CCN). At a water vapour saturation ratio just above 100%, the CCN are no longer in the equilibrium domain. Instead, the CCN are *activated* into cloud droplets and grow unrestrained as long as there is water vapour available for condensation. In warm clouds, these particles may grow via condensation from sizes of about 100 nm to cloud droplets of about

10-20 µm within 1-20 min (Lamb and Verlinde, 2011). In Figure 1, the typical sizes of particles, cloud droplets and raindrops are illustrated. The cloud droplets can either continue to grow into raindrops, or evaporate to form particles and water vapour again, depending on their environmental conditions. Typical cloud droplets (~20 µm in diameter, depending on the kind of cloud) can grow into typical raindrops (~2000 µm) in about 30 min, depending on the initial drop spectrum and availability of water in their surroundings (Lamb and Verlinde, 2011). On average, only every tenth of a cloud droplet become a rain droplet, while the rest evaporate (Rodhe, 1992).

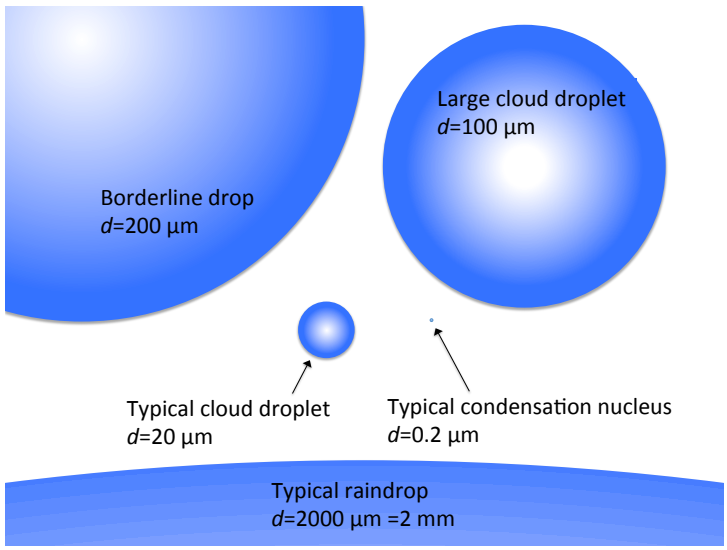

Figure 1. Typical sizes of particles, cloud droplets and raindrops
Comparison of droplets with different sizes (*d*, diameter) present in the atmosphere.

Anthropogenic emissions

The London smog of 1952 (Brimblecombe, 1978) is one of the most famous events associated with soot emissions. The severity of the effects of the soot emissions from burning coal on human health resulted in the control and improvement of pollution levels, as well as the development of the first techniques for the measurement of soot concentration (Thomas, 1952; Wilkins, 1954). After the reduction in soot concentration, in combination with an increase in consumption of other fuels (primarily petrol), the research was directed towards aerosol formation through photochemical gas-to-particle conversion processes in the atmosphere (Novakov and Rosen, 2013). The air pollution that arises as a result of petrochemical-based fuels forms a different kind of smog, in places like Los Angeles, resulting in poor visibility and eye irritation. This smog, primarily

produced from photochemical ageing of the nitrogen oxides and hydrocarbons in traffic exhausts, differs in content and concentration depending on the physical location and meteorological conditions. Smog is also affected by inorganic compounds such as salts (sodium chloride, sulphates and nitrates), soot and minerals, as well as thousands of organic compounds already abundant in the atmosphere. In many places, up to 90% of the submicron aerosol mass is organic material (Jimenez et al., 2009; Kanakidou et al., 2005), and secondary organic aerosol (SOA) makes up a substantial part of it. The SOA is a product of the oxidation and condensation of volatile gas-phase hydrocarbons, from both anthropogenic and biogenic sources, into the particle phase. Biogenic SOAs make up for 50-70% of the total organic aerosol budget, and the production of biogenic SOA can be enhanced when it is co-emitted with precursors from anthropogenic sources (Carlton et al., 2010; Hoyle et al., 2011; Shilling et al., 2013; Spracklen et al., 2011). An increase in the proportion of organic material in a particle changes its properties, and may enhance its ability to take up water, however, inorganic salts have a greater effect on water uptake.

In the late 1960s and early 1970s, attention was once again directed towards soot particles as measurements of urban aerosols indicated that soot could constitute a substantial part of the atmospheric aerosol. Soot particles account for a large fraction of the atmospheric aerosol number concentration, especially in the size range below 100 nm, in urban locations (Rose et al., 2006 and references therein). Soot particles are produced as a by-product during combustion processes, and consist mainly of a black carbon (BC, the light-absorbing fraction) component and an organic component, both emitted from the source (Novakov and Rosen, 2013; Petzold et al., 2013). The largest sources of ambient soot are the combustion of fossil fuel, fuels from industrial and residential use, and biomass burning. Soot particles may have various shapes, sizes and composition, which can change during retention in the atmosphere (Figure 2). Soot particles consist of hydrophobic spherules of about the same size, connected by weaker and/or stronger bonds (van der Waals forces and/or covalent bonds, respectively) (Tree and Svensson, 2007).

Figure 2. TEM images of (a) fresh and (b) photochemically processed soot particles.
The freshly emitted soot particle has a more agglomerated structure, while the particle that has aged for 2 hours is more compact. The soot particles were produced from diesel exhaust and anthropogenic SOA precursors.

Freshly emitted diesel exhaust nanoparticles and burner soot from a laboratory-generator are hydrophobic, i.e. they have limited hygroscopicity and show little or no restructuring when exposed to water vapour (Pagels et al., 2009; Tritscher et al., 2011; Weingartner et al., 1997; Zuberi et al., 2005). These primary emissions of soot are unlikely to act as CCN in the atmosphere. However, during photochemical processing of the soot nanoparticles in the atmosphere (i.e. exposure to UV radiation, ozone, radicals, condensation of organic and inorganic compounds (Rose et al., 2006) and the coagulation of other particles onto the agglomerates), the physical and chemical particle properties change leading to restructuring (Figure 2 b) and an increase in water vapour uptake (e.g. Ma et al., 2013; Pagels et al., 2009; Tritscher et al., 2011; Weingartner et al., 1997; Zhang et al., 2008). The increase in hygroscopicity depends on the ageing time, type of combustion process, type of fuel (levels of content of impurities such as sulphur, e.g. Gysel et al. (2003)), and volatile organic compounds (VOCs) present in the emissions and the environment. According to Schnitzler et al. (2014), the restructuring of the soot core will start after the condensation of a high amount of material (increase in mass by a factor of ~2). Furthermore, the soot core can only restructure to a certain degree, resulting in a non-spherical shape (shape factor, χ, of ~1.8, further described at p.23), and the spherical-like shape is obtained by the filling of cavities and voids with condensing material. The degree to which the restructuring occurs has not been fully investigated, and may depend, for example, on the type of soot produced (more or less porous depending on the combustion process and fuel used), the type of condensing material (including properties such as surface tension, density, and polarity), and whether the condensing material is in the liquid or solid phase.

Measurement Techniques

Experimental outlines in laboratory and field

Experiments were performed on the photochemical processing of traffic exhausts (particles and precursors) in the Aerosol Laboratory smog chamber at Lund University (Papers I, II, and IV). Black lights with a peak at 354 nm were used to induce the photochemical ageing of particles in the 6 m^3 Teflon/FEP chamber. The hygroscopic properties of the particles were measured using cloud condensation nuclei counters (CCNC) and a hygroscopic tandem differential mobility analyser (H-TDMA). The transformation of the ageing particles was studied using a differential mobility analyser in conjunction with an aerosol particle mass analyser (DMA-APM), an aerosol mass spectrometer (AMS), a scanning mobility particle sizer (SMPS), an aethalometer, and transmission electron microscopy (TEM) were used. These instruments are described in more detail in the following sections.

In the first study (Paper I), the exhaust (particles and SOA precursors) from a Euro II diesel private vehicle and particles from a flame soot generator were aged by adding various amounts of toluene and *m*-xylene as precursor sources, and the hygroscopicity in the supersaturated regime and the restructuring of the soot particles were studied.

In the second study (Paper II), the water vapour uptake of a SOA was studied. The SOA were produced from the precursors in the diesel exhaust in combination with the precursors mentioned above, or the added precursors only, or from gasoline exhaust (two different gasoline passenger vehicles: Euro II and IV). Soot particles (diesel soot or soot from a flame soot generator) or ammonium sulphate (AS) particles were used as seed particles for the condensation of the SOA.

Field measurements were performed on an urban aerosol in a street canyon in central Copenhagen (Papers III, and IV), and on a rural aerosol at a background measurement station, at Vavihill in the southern Sweden (Paper IV). The instruments listed above were used for the field measurements with the exception of TEM and the H-TDMA, which were not used at the rural station. In addition, an aethalometer was used at both sites.

The cloud condensation nuclei counter

CCNCs can be used for measurements of the cloud activation properties of the particles, i.e. particle water vapour uptake under supersaturated conditions. In this work, the CCNC (DMT-100) was operated in two ways: 1) in the traditional manner as a continuous-flow streamwise thermal-gradient CCNC (CFSTGC-CCNC, Lance et al., 2006; Roberts and Nenes, 2005), or 2) using scanning flow CCN analysis (SFCA, Moore and Nenes, 2009), as illustrated in

Figure 3.

The instrument is based on the principle that the diffusion of heat is slower than the diffusion of water vapour in air. There is a vertical thermal gradient through a continually wetted column. As the particles travel along the symmetry axis at the centre of the column (under continuous flow) surrounded by sheath air, the temperature and water vapour concentration to which the particles are exposed will depend on the distance from the walls upwind (see

Figure 3). Due to the difference in diffusion velocity more water vapour will be available than is thermodynamically allowed, and supersaturation will be achieved. An optical particle counter is used to count the particles that have taken up enough water vapour for the particles to be detected. According to the manufacturer, the instrument can be set to levels of supersaturation ranging from 0.07 to 2%. The residence time in the CCNC is 6–12 s.

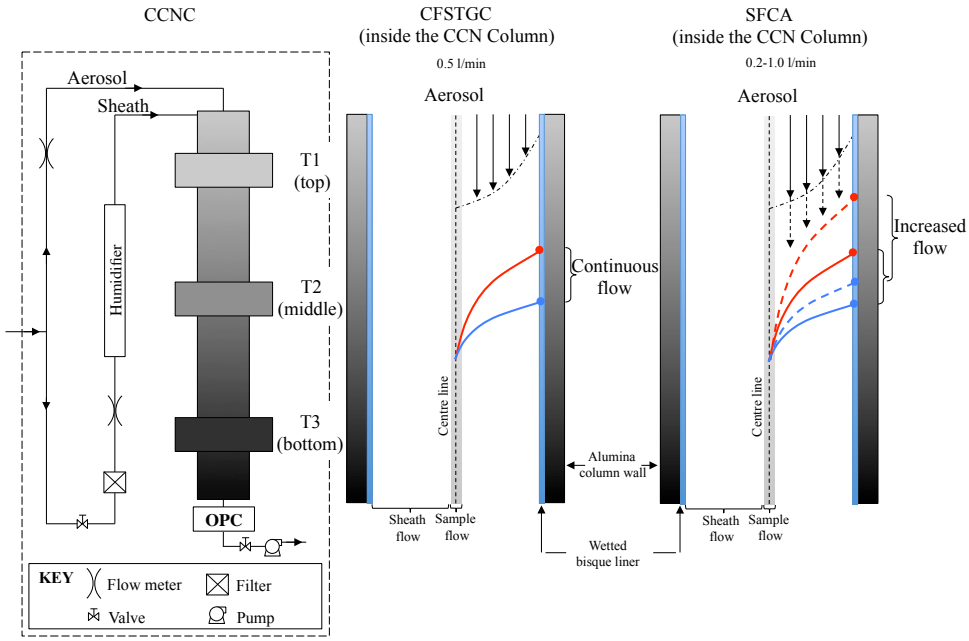

Figure 3. The working principle of the CCNC
A schematic of the CCNC is shown within the dotted lines on the left. The image in the centre illustrates how supersaturation is generated in the CCNC column when the instrument is operated in a traditional manner (CFSTGC) and in the right-hand image in scanning flow mode (SFCA). The diffusion of water vapour is shown in blue, and the diffusion of heat in red. The aerosol sample at the centre line is subjected to a high level of water vapour, i.e. the particles are exposed to supersaturation. To change the degree of supersaturation in CFSTGC mode, the temperature gradient (ΔT: T3-T2-T1) through the column is changed, using a constant total flow (sheath+sample air). When using SFCA mode, a change in flow through the column will generate a change in supersaturation at a constant value of ΔT. As the flow increases (decreases), the distance between the starting points for the heat (dashed red line) and water vapour (dashed blue line) will increase (decrease), hence varying the supersaturation. The change in the flow through the column is much faster than the change of the temperature gradient.

During the work presented in Paper I, the CCNC was firstly operated in the traditional manner, with the DMA placed before the instrument to enable size selection based on the mobility diameter (d_z) of the dry monodisperse aerosol particles. During these measurements, the change in supersaturation was induced in a "conventional" manner (for a critical supersaturation, $s_c < 1$ %). The flow (Q) and d_z were kept constant, while the temperature gradient (ΔT) was varied stepwise. Measurements of complete supersaturation spectra using this set-up are time consuming due to the slow temperature stabilisation. Therefore, the SFCA mode of operation was implemented, which enables rapid, continuous measurements of the supersaturation spectra, by implementing small changes in the software of the CCNC. The SFCA mode was used in the work presented in Papers I, II, III, and V. In the SFCA mode, the total flow (sheath and sample air) is varied through the column in a controlled manner, while the streamwise ΔT and pressure (P) are kept

constant. The level of supersaturation is increased by increasing the flow, which in turn increases the travel distance between the water and heat to the centre line/particle. The flow rate in the chamber is increased or decreased linearly, and kept constant at the maximum and minimum flow rates in between. The scan cycle determines the resolution of the measurement, and was set to ~5 min, and ΔT was chosen depending on the saturation ratio required for the specific aerosol, i.e. the scan cycle and ΔT are measurement specific. For example, a short cycle is used for airborne measurements and fast ageing, and longer scan cycles when high resolution is required, and a high temperature gradient is used for less hygroscopic species and/or small particle diameters. Each calibration curve is specific for the chosen values of ΔT, P and scan cycle time. The s_c is derived from the flow rate. The flow rates and the corresponding CCN number concentrations generate a supersaturation curve, with a "critical flow rate" (Q_{50}). Q_{50} is translated into the value of s_c using Köhler theory and knowledge of the chemical composition and diameter of the dry particle (d_s), i.e. every instantaneous flow rate corresponds to a level of critical supersaturation. Using SFCA mode instead of CFSTGC mode increases the temporal resolution and reduces the amount of sample required for analysis. According to Moore and Nenes (2009), because ΔT is kept constant, and therefore close to ambient temperature, using SFCA mode also minimizes biases resulting from the volatilization of semi-volatile compounds.

The CCNC (using CFSTGC or SFCA mode) was calibrated using a solution of well-known chemistry for the generation of a size-selected aerosol, according to the guidelines of Rose (2008). AS was usually used as the calibration solution in this work. However, to obtain reliable calibration curves for the highest levels of supersaturations needed when running in SFCA mode (i.e. the highest values of ΔT=18 K), sucrose was successfully used for calibration. One of the advantages of using sucrose as the calibration solution is that, for a specific particle diameter, the sugar particles become activated at significantly higher levels of critical supersaturations than salts (Rosenørn et al., 2006). Furthermore, sucrose has non-dissociative (van't Hoff factor, i=1) and non-volatile properties. A disadvantage of the sucrose is that it is difficult to obtain sufficiently dry sucrose particles after generation in the atomizer. The calibration curves for the CFSTGC measurements were obtained by either changing the level of supersaturation, or the particle diameter stepwise. A relaxed step function was fitted to the calibration curve, revealing the critical supersaturation or the critical diameter at the point where 50% of the particles were activated (Svenningsson and Bilde, 2008). In the SFCA measurements, the calibration curves were obtained by changing the flow rate (as described above). A sigmoidal function was fitted to the calibration curve, in a similar way to the CFSTGC. However, in the SFCA mode, the flows and corresponding activated fractions generate a supersaturation curve resulting in a Q_{50} that is translated into s_c using Köhler theory (as discussed above). Figure 4 illustrates

the calibration functions where every Q_{50} corresponds to a s_c, which were obtained from the sigmoidal calibration curves.

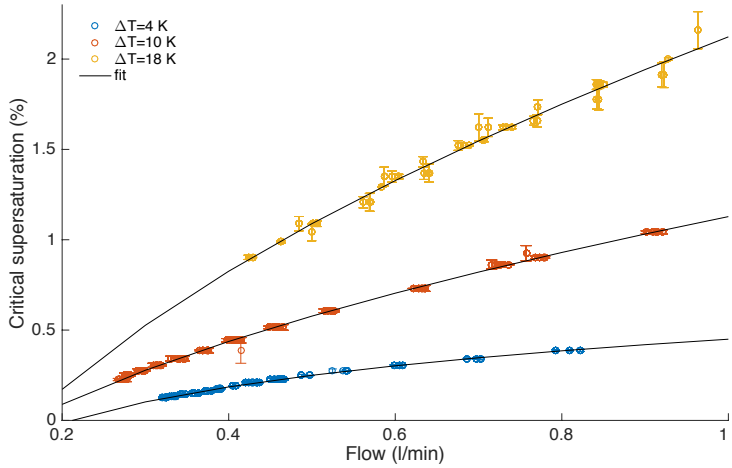

Figure 4. Calibration functions for the convertion of critical flow (Q_{50}) to critical supersaturation (s_c) Example of calibration functions obtained from SFCA measurements of AS particles. Each data point corresponds to a calibration curve, where the Q_{50} corresponds to the flow rate at which 50% of the paticles are activated. Each value of Q_{50} is translated into a level of supersaturation using Köhler theory, together with knowledge of the solution chemistry and dry particle diameter.

In order to handle the higher data load resulting from the SFCA procedure, I developed a program using MATLAB. This program was used for evaluation of the data presented in Papers I, II, and III.

The CCNC was operated in the CFSTGC mode while measuring the polydisperse, ambient aerosol at the Vavihill rural measurement station (Paper IV).

The hygroscopic tandem differential mobility analyser

An H-TDMA can be used for measurements of the particle water vapour uptake under subsaturated conditions, by measuring the hygroscopic growth factor, as described in detail by Fors et al. (2011); and Nilsson et al. (2009). Particles with a well-defined size are first selected according to their mobility diameter using a DMA (Vienna type, 28 cm long). The dry monodisperse aerosol is then conditioned by exposure to a defined RH. The mean diameter of the conditioned aerosol size distribution (*d(RH)*) is then determined, using a second DMA (Vienna type, 50 cm long, and an RH of 90%,) and a condensation particle counter. The H-TDMA was calibrated using ammonium sulphate (AS) particles, and the data inversion was performed using the TDMAinv method (Gysel et al., 2009). The hygroscopic growth factor (*gf*), defined as $d(RH)/d_s$ (where d_s=d_z) could then be determined. The H-TDMA was used for the analysis discussed in Papers II-V.

Auxiliary instrumentation

The aerosol particle mass analyzer (APM)

A DMA-APM setup (model 3600, Kanomax, Japan; McMurry et al., 2002) was used to characterize the mass-mobility relationship of single particles, as described by Rissler et al. (2013). By introducing a thermodenuder between the DMA and APM it was possible to quantify the size-dependent mass fraction between volatile and non-volatile species in the particle, as well as the effective density of the particles. The approach of comparing measurements with and without a thermodenuder (TD) was introduced by Pagels et al. (2009).

Aerosol mass spectrometer

An online aerodyne high-resolution time of flight aerosol mass spectrometer (HR-ToF-AMS, Aerodyne Research, USA) was used to obtain information on the chemical composition of aerosol particles. The measurements performed with this instrument sizes the particles with respect to the vacuum aerodynamic diameter, and the performance is good in the size range ~50-500 nm. The instrument was further equipped with a laser vaporizer, for the detection of refractory black carbon (soot particle aerosol mass spectrometer, also from Aerodyne Research) and was used for measurements on soot cores. For detailed descriptions of both instruments see DeCarlo et al. (2006) and Onasch et al. (2012). The AMS set-ups were used in all the studies described in Papers I-V.

Aethalometer

A seven-wavelengths aethalometer (370, 470, 520, 590, 660, 880, 950 nm) (AE33, Magee Scientific, USA) was used for the light absorption measurements presented in Papers III, IV and V. Briefly, the polydisperse aerosol is deposited on a filter and irradiated by seven LEDs. A photodetector is used to measure the light attenuation, which increases with increasing particle deposition. The instrument has been described in detail by Drinovec et al. (2015).

Scanning mobility particle sizer

The particle number size distribution was measured in the range d_z=10-600 nm, using an SMPS system (custom built; Löndahl et al., 2008). The SMPS system includes a ^{63}Ni bipolar charger, a DMA (Vienna type, 28 cm long), and a condensation particle counter (model 3010, TSI Inc., USA) and has a sheath-to-aerosol flow ratio of ~7.

Transmission electron microscopy

High-resolution transmission electron microscopy (HR-TEM) image analysis was used to determine the primary particle size and microstructure of the soot particles (as described in Papers I, II, and V). Briefly, the soot agglomerates were deposited onto TEM grids (lacey carbon coated copper) using an electrostatic precipitator (NAS model 3089, TSI Inc., operated at 9.6 kV, at an air flow rate of 1 l/m). The samples were then analysed using HR-TEM (JEOL 3000 F, 300kV) equipped with a field emission gun. This analysis was performed by others, and is described by Rissler et al. (2013).

Data Analysis

Particle water vapour uptake

Modification of Köhler-theory to take water solubility into account

Cloud droplets form in the atmosphere by the condensation of water vapour onto CCN. Growth of the cloud droplet is favoured by a high saturation ratio (s>100%), larger particles, and more soluble material in the particle core. Hence, the number of non-dissociating molecules or ions per unit volume of the dry particle, which varies with size and chemical composition, will determine the critical water vapour supersaturation at which the particles become activated and form cloud droplets. Soluble material in the particle core also attracts water at subsaturated conditions (s<100%). At subsaturation, droplets of supersaturated salt solutions (e.g. AS) can exist, and at saturation ratios of 95% most of the mass of the salt solution droplet is water. In the subsaturated regime, the water vapour uptake of the particle is often described by the growth of the particle, i.e. by the hygroscopic growth factor. The growth of the droplet will also be affected by the curvature of the droplet surface, which will change the saturation vapour pressure acting over the surface. As water evaporates from the droplet, the diameter will decrease, while the curvature increases. As the curvature increases, water molecules at the surface will have fewer and fewer neighbours, making it easier for the molecules to escape.

In 1936 Professor Hilding Köhler combined the effects of water activity and curvature to describe the growth of a dry particle into a cloud droplet by condensation of water. In Köhler theory the saturation ratio, s, over an aqueous solution droplet is defined as the ratio of the actual partial pressure of water (p) and the equilibrium pressure over a flat surface of pure water (p_0), acting at the same temperature (Pruppacher and Klett, 1997; Seinfeld and Pandis, 2006), hence:

$$s = \frac{p}{p_0} = a_w * Ke \qquad \text{Eq. (1)}$$

where Ke represents the Kelvin effect or curvature describing the higher partial pressure due to the curved surface of the droplet compared to a flat surface, and is defined as:

$$Ke = \exp\left(\frac{4\sigma_{s/a}M_w}{RT\rho_w D}\right) \quad \text{Eq. (2)}$$

where $\sigma_{s/a}$ denotes the surface tension of the solution/air interface, which is temperature-dependent, but assumed here to have a constant value, equal of that for water (0.072 J m^{-2}), R denotes the universal gas constant, T is the absolute temperature, and D is the diameter of the spherical aqueous solution droplet. ρ_w and M_w and are the molar density and the molecular weight of water, respectively. The following form of Raoult's law was used to calculate the water activity (a_w), including the Zdanovskii, Stokes, and Robinsson (ZSR) mixing rule:

$$a_w = \frac{n_w}{n_w + \sum_s i_s n_s} = \left(1 + \sum_s i_s \frac{n_s}{n_w}\right)^{-1} = \left(1 + \frac{n_{sum} M_w}{\rho_w \frac{\pi}{6}\left(D^3 - d_{dry}^3\right)}\right)^{-1} \quad \text{Eq. (3)}$$

where n_w and n_s are the number of moles of water and component s, respectively. i_s is the van't Hoff factor, which expresses that the substance s takes up water as if it forms i_s moles of soluble species per mole solute. The dry particle diameter is denoted by d_{dry}. The ZSR mixing rule assumes that the uptake of water by each separate compound is independent of the other constituents of the particle, i.e. n_{sum} is the sum of the number of moles from all components in the particles, defined as:

$$n_{sum} = \sum_s \frac{\varepsilon_s i_s \rho_s d_{dry}^3}{M_s} \frac{\pi}{6} \quad \text{Eq. (4)}$$

where ε_s is the volume fraction of a component s in a dry particle with diameter d_{dry}, and ρ_s and M_s denotes the density and molar mass of the component s, respectively. This was used in the study described in Paper I.

In a later study (Paper II), a modified version of the traditional Köhler theory (adopted from Bilde and Svenningsson, 2004) was used to account for limited solubility of the particle core material. If the material in the particle core has limited water solubility, the water vapour uptake may differ from that predicted by traditional Köhler theory (Bilde and Svenningsson, 2004; Broekhuizen et al., 2004; Huff Hartz et al., 2005; Kulmala et al., 1997; Raymond and Pandis, 2002; Shulman et al., 1996). Here, the organic material in the core is divided into two components: 1) one that is infinitely soluble in water, and 2) a second that has limited water solubility. Due to solubility limitation, undissolved organic material will be present in the core, until sufficient water has condensed onto the particle. This is a simplification, as in reality the two components defined above represent numerous

organic compounds, with different solubilities. However, these are difficult to determine both in the laboratory and under ambient conditions. The amount of substance available to take up water is determined by:

$$n_s = min\left\{\frac{(D^3 - {d_{dry}}^3)C_{sat,s}}{M_s} \middle| \frac{\beta_s \rho_0 {d_{dry}}^3}{M_s}\right\}\left(\frac{\pi}{6}\right) \quad \text{Eq. (5)}$$

where:

$$\frac{1}{\rho_0} = \sum_s \frac{\beta_s}{\rho_s} \quad \text{Eq. (6)}$$

β_s denotes the mass fraction of compound *s* in the initial dry particle. $C_{sat,s}$ is the solubility (mass per unit volume) of compound *s* in water, and ρ_0 is the density of the dry particle, given by Eq. (6), assuming volume additivity. The modified version (implementing Eq. (5) in equation (1)) will correspond to traditional Köhler theory when sufficient water has condensed on the particle to dissolve all the organic material.

Figure 5 illustrates the water uptake of a spherical organic particle, where component 1 is infinitely soluble in water and component 2 has limited solubility. In Figure 5a-c the solubility is varied ($C_{sat,2}$=1, 10, 1000, 5000, ∞ g l^{-1}), while the two components of the organic fraction are kept constant (β_1=1-β_2, and β_2=0.6). In Figure 5d-f the solubility is kept constant ($C_{sat,2}$=10 g l^{-1}), while the fractions are varied (β_1=1-β_2, and β_2=0.2, 0.4, 0.6, 0.8, 1). Water vapour uptake differs depending on the water vapour available in the surrounding environment, i.e. the saturation conditions, and also which parameter is varied ($C_{sat,s}$ or β_s). Figure 5a and 5d illustrate the total water vapour uptake (the Köhler curve, denoted as *s*) as well as the two competing effects, i.e. the water activity (a_w) and the Kelvin effect (*Ke*). In Figure 5b and 5e only the case for the supersaturated regime is shown. The modified Köhler theory, shown by the red line ($C_{sat,2}$=10 g l^{-1} and β_2=0.6) predicts two maxima. The first supersaturation maximum ($s_{c,1}$) constitutes an activation barrier, and is affected by both the magnitude of $C_{sat,2}$ and the amount of material (β_2). At this maximum, part of the organic material of component 2 has not dissolved, and will not be dissolved until the diameter of the droplet corresponds to the cusp at the curve. The value of $s_{c,1}$ converges towards the value of $s_{c,2}$ (the second maximum), with increasing values of $C_{sat,2}$ and/or decreasing values of β_2. The limited water vapour uptake is more pronounced in the subsaturated regime, presented in Figure 5c and 5f.

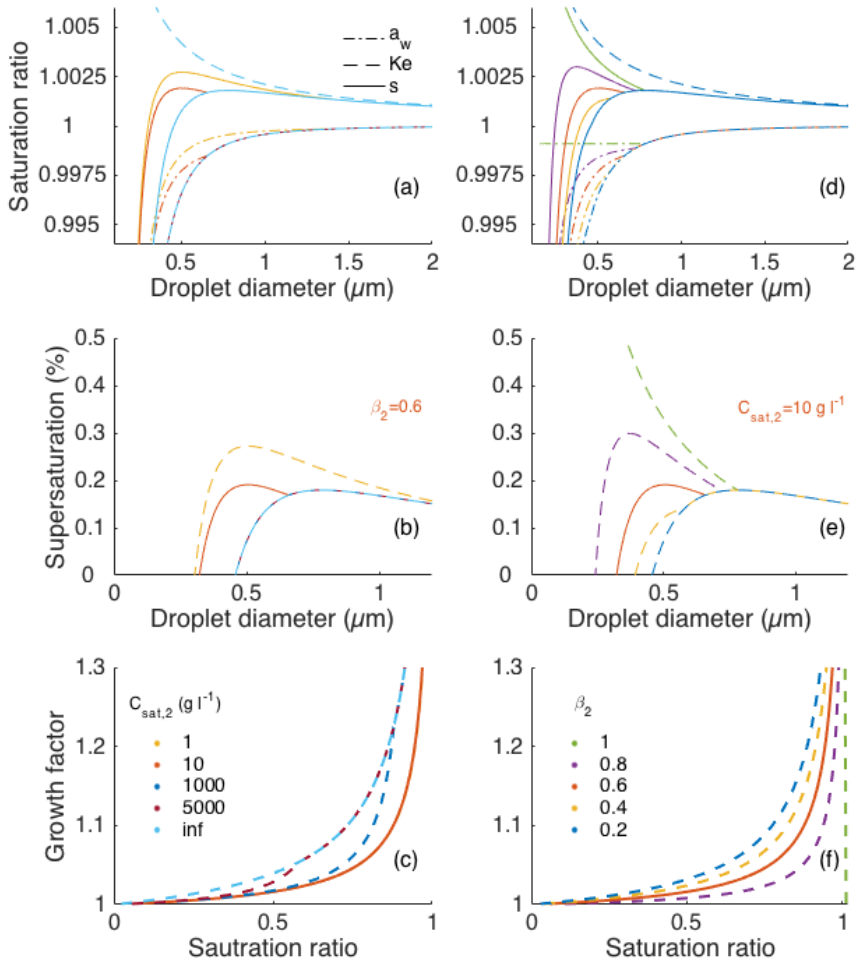

Figure 5. Köhler curves modified to take water solubility limitation into account
Modified Köhler theory is used here to illustrate the water uptake of a spherical organic particle with a dry size of 150 nm. In (a)-(c) the solubility ($C_{sat,2}$) is varied, while the fraction of the organic maeterial with a limitited solubility(β_2) is kept constant at 0.6. In (d)-(f) β_2 and $C_{sat,2}$ is kept constant at 10 g l^{-1}. The red line denote Köhler curves with the same input values ($C_{sat,2}$=10 g l^{-1} and β_2=0.6). (a) and (d) show the water activity (a_w), the Kelvin effect (Ke) and the saturation ratio (s=a_w*Ke) as a function of droplet diameter. (b) and (e) show the supersaturation as a function of droplet diameter, and (c) and (f) show the growth factor with respect to the saturation ratio. Note, that in the supersaturated regime (a) and (b) for the values used, the results for $C_{sat,2}$>1000 g l^{-1} follow the same Köhler curve, and in the subsaturated regime (c) the results for $C_{sat,2}$<10 g l^{-1} follow the same curve.

κ-Köhler theory

The water activity can be represented in a more succinct form by the hygroscopicity parameter, κ (Petters and Kreidenweis, 2007; Rissler et al., 2006). This parameter is widely used for direct comparisons between subsaturated and supersaturated conditions, i.e. for comparing the results from the H-TDMA and the CCNC. Rissler et al. (2006) were the first to introduced an H-TDMA-derived form of κ, which gave the number of non-dissociating molecules or ions in the dry particle, per unit volume. Later, Petters and Kreidenweis (2007) introduced a similar parameter, differing only in the choice of units (Rissler et al., 2010). In the work described in this thesis, the more broadly used parameter introduced by Petters and Kreidenweis (2007) was used. κ is related to the saturation ratio, s, over an aqueous solution droplet as follows:

$$s(D) = \frac{D^3 - d_{dry}^3}{D^3 - d_{dry}^3(1-\kappa)} \exp\left(\frac{4\sigma_{s/a} M_w}{RT\rho_w D}\right). \quad \text{Eq. (7)}$$

The maximum value of Eq. (7) is the s_c. From knowledge of the dry particle diameter and the corresponding value of s_c from CCNC measurements, κ_{CCN} can be approximated for κ>0.2 by:

$$\kappa_{sc} = \frac{4A^3\sigma_{s/a}^3(T)}{27T^3 d_{dry}^3 ln^2 S_c}, \quad \text{Eq. (8)}$$

where $A = \frac{4M_w}{RT\rho_w}$. If small numerical errors are acceptable, Eq. (8) can be used for values of κ above ~0.01 (Petters and Kreidenweis, 2007). For low values of κ (i.e. below 0.2), the behaviour of the particle will be non-ideal, i.e. the initial dry particle volume can contribute to the total volume of the droplet such that the water vapour uptake will approach that expected for an insoluble but wettable particle (as predicted by the Kelvin equation alone).

Rearrangement of Eq. (7) allows κ_{gf} to be calculated from the hygroscopic diameter growth factor as a function of relative humidity, from measurements made using the H-TDMA:

$$\frac{RH/100\%}{exp\left(\frac{4\sigma_{s/a}M_w}{RT\rho_w d_{dry} gf}\right)} = \frac{gf^3 - 1}{gf^3 - (1-\kappa_{gf})} \quad \text{Eq. (9)}$$

Alternatively, the overall value of κ can be calculated from the chemical components and corresponding volume fractions in the particle, using the ZSR mixing rule:

$$\kappa_{chem} = \sum_s \varepsilon_s \kappa_s \quad \text{Eq. (10)}$$

where

$$\kappa_s = i_s \left(\frac{\rho_s M_w}{\rho_w M_s}\right) \quad \text{Eq. (11)}$$

κ_{chem} can be inserted into Eq. (7) for predictions of the particle water content and relative humidity in the subsaturated regime, as well as predictions of the activation into cloud droplets. κ ranges from 0 for non-hygroscopic compounds, to approximately 1.4 for highly CCN active salts, respectively (Petters and Kreidenweis, 2007). Empirically derived values of κ are summarized in Table 1.

Table 1. κ values

κ values for aerosols of different origin, derived from measurements in the subsaturaded (H-TDMA) and supersaturated regimes (CCNC).

Compounds	κ value/ range	Reference
Non-hygroscopic compounds	0	Petters and Kreidenweis (2007)
Slightly to very hygroscopic organic species	0.01-0.5	Petters and Kreidenweis (2007)
Highly CCN-active salts (e.g. NaCl, AS)	0.5-1.4	Petters and Kreidenweis (2007); Ruehl et al. (2010)
Ambient particles, marine aerosol (many locations)	0.6-0.9	e.g. Andreae and Rosenfeld (2008 and references therein); Poschl et al. (2009)
Ambient particles, urban and continental aerosol (many locations)	0.2-0.3	e.g. Andreae and Rosenfeld (2008); Poschl et al. (2009); Rose et al. (2010)
Laboratory-aged anthropogenic SOA (precursors: lubrication oil)	0-0.02	e.g. Lambe et al. (2011); Lide (2005)
Laboratory-aged anthropogenic SOA (precursors: diesel exhaust aerosol)	0-0.14	e.g. Gysel et al. (2003); Kuwata et al. (2013); Tritscher et al. (2011)
Laboratory-aged anthropogenic SOA (precursors: *m*-xylene, p-xylene, benzene, toluene, trimethylbenzene)	0.04-0.27	e.g. Prenni et al. (2007); Jimenez et al. (2009); Lambe et al. (2011); Zhao et al. (2016); Guo et al. (2016)
Laboratory-aged biogenic and anthropogenic SOA mixture (precursors: α-pinene, limonene, p-xylene, toluene)	0.03-0.14	Zhao et al. (2016)
Laboratory-aged biogenic SOA (precursors: α-pinene, β-caryophyllene, isoprene, β-pinene, Δ^3-carene)	0.002-0.18	Asa-Awuku et al. (2009); Duplissy et al. (2008); Frosch et al. (2013); Jimenez et al. (2009); Petters et al. (2009); e.g. Prenni et al. (2007); Zhao et al. (2015)
Ambient particles in urban areas, North American continent (Canada, Mexico and US west coast)	0.04-0.51	Chang et al. (2010); Jimenez et al. (2009); Shinozuka et al. (2009)
Ambient particles in rural areas, European continent (Switzerland, Finland, Germany)	0.12-0.46	Jimenez et al. (2009); Wu et al. (2013)
Ambient particles in rural areas, South American continent (Amazon)	0.10-0.22	Gunthe et al. (2009)
Ambient particles in urban areas, European continent (France)	0.08-0.27	Juranyi et al. (2013)
Biomass burning	0.01-0.55	Andreae and Rosenfeld (2008)
Wood burning particles: fresh and aged	0-0.39	Martin et al. (2013); Zhao et al. (2015)

Discrepancy in hygroscopicity under subsaturated and supersaturated conditions

Petters and Kreidenweis (2007) compared κ values derived from the two measurement techniques, CCNC and H-TDMA). For most of the 25 compounds examined, the agreement was within 30%. However, the difference between κ_{CCN} and κ_{gf} can be greater (e.g. Fors et al., 2010; Zhao et al., 2016). Some of the disagreement can be attributed to the measurement techniques, although this does not explain the considerable difference in the values of κ measured under subsaturated and supersaturated conditions. There are other examples in the literature of discrepancies in κ (Martin et al., 2013; Tritscher et al., 2011; Zhao et al., 2015), and it has been suggested that this may be due to bulk-to-surface partitioning of surface-active compounds, incorrectly assigned surface tension and solubility limitations (e.g. Bilde and Svenningsson, 2004; Hodas et al., 2016; Petters and Kreidenweis, 2013; Ruehl et al., 2010; Wex et al., 2009).

Definition of aerosol diameters

Particle diameter is an important property that determines, for example, the transportation characteristics and lifetime of the particle in the atmosphere, their light scattering and absorption, and their deposition in the respiratory tract. A wide range of instruments have been developed to measure particle concentrations (e.g. based on number, mass, volume or chemical composition) as a function of particle size (DeCarlo et al., 2004, and references therein). However, the particle size, or diameter, can be defined in different ways, and differs depending on the production process. Combustion, gas-to-particle conversion, and condensation processes produces particles with different morphologies. Furthermore, the selection and measurement of the particle of a specific size will differ depending on the technique used. For instance, the flow regime of the gas around the particle in the instrument will affect the measurements (as described in more detail below). A DMA, for example, measures the electrical mobility diameter (d_z), while an AMS measures the vacuum aerodynamic diameter (d_{va}). Measurements performed simultaneously by mobility and aerodynamic techniques on non-spherical particles (or non-unit density particles) (Figure 6a and b), such as agglomerated diesel soot particles, will show substantial differences in size distributions when using techniques based on mobility and aerodynamics. These differences are not true discrepancies, but arise from different definitions of particle diameter. Important information can therefore be obtained by comparing the results of measurements using different techniques. It is therefore important to describe the particle diameter using a common parameter. It is possible to derive a coherent mathematical description of the particles by combining information on the density and morphology obtained from different measurements of the equivalent diameter (d_z and d_{va}). In this thesis, the volume equivalent diameter (d_{ve}; related to the dynamic shape factor, χ) was derived from measurements of the mass-mobility relationship and used to study the particle

behaviour (Paper I). The relationship between the three diameters can be condensed into the following form (for a detailed review see DeCarlo et al., 2004);

$$\frac{d_z}{C_c(d_z)} = \frac{d_{ve}\chi_t}{C_c(d_{ve})} = \frac{\frac{d_{va}\chi_v\chi_t\rho_{st}}{\rho_p}}{C_c(\frac{d_{va}\chi_v\rho_{st}}{\rho_p})}, \quad \text{Eq. (12)}$$

where C_c represents the empirical Cunningham slip correction factor (which differs for the different equivalent diameters of the same particle). χ_t and χ_v denotes the shape factor in the transition regime and the vacuum or free molecular regime, respectively (the different regimes are described below). ρ_{st} is the standard density (1000 kg m^{-3}) and ρ_p is the particle density (including preserved internal void spaces as a phase with zero density). The shape factor for spheres is 1 (i.e. d_z=d_{ve}), and for highly agglomerated particles such as fresh soot, χ>2, and is size dependent.

The flow regime in the instrument is important when the particles are size-selected via the ratio of the drag force (i.e. that exerted by the gas molecules on the particles) to some other force exerted on the particles. The drag force will affect the particles differently depending on flow regime, particle size and shape (see e.g. DeCarlo et al., 2004; Hinds, 2012). The main flow regimes are: the 1) *continuum*, 2) the *transition* and the 3) *free-molecular* regime. In the first, the gas flows around the particle like a continuous fluid, while in the third, the particles may collide with the gas molecules. The flow in the transition regime is in between that in regimes 1) and 3).

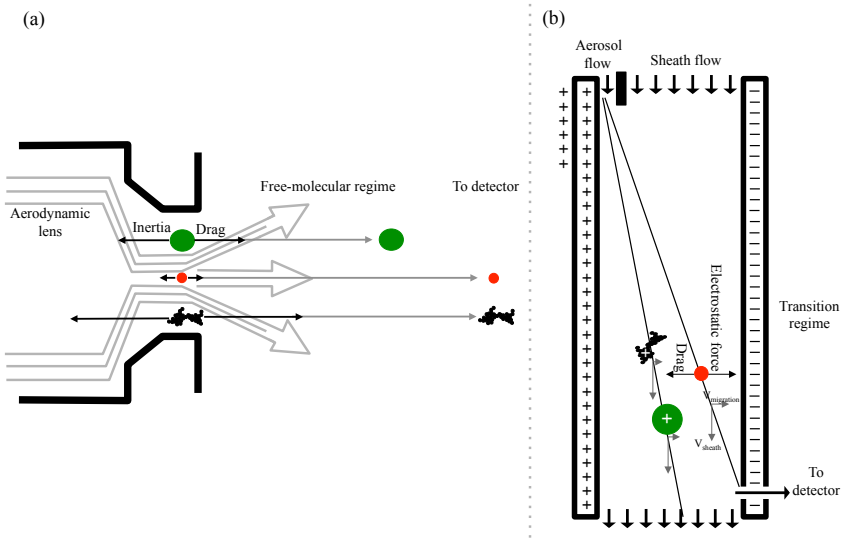

Figure 6. Particle motion in an AMS and a DMA
Illustration of particle motion, depending on the size and shape of the particle, moving in an AMS (a) and a DMA (b). In the AMS, the irregular particles have the same mass as the larger of the two spherical particles and move with the same velocity with which the smaller spherical particles leave the nozzle, indicated by the grey arrows. In the DMA, irregular particles move with the same velocity as the larger spherical particles, but have the same mass as the smaller spherical particles.The grey arrows show the velocity vectors for electrical migration (vertical) and the sheath flow (horizontal). (Adapted from DeCarlo et al., 2004).

Figure 6 illustrates particles of different size and shape, moving in an AMS and a DMA. In an AMS, particles travel in the free-molecular regime, and the drag force is balanced by particle inertia. At the end of an aerodynamic lens, the particles acquire a size-dependent velocity during supersonic expansion into vacuum. In a DMA, an electrical force exerted on the particles balances the transition regime drag force. The migration velocity of a spherical particle with a certain diameter in a constant electric field defines the electrical mobility diameter of the particle.

Even if the physical morphology is the same, the density of the particles (i.e. the composition) will affect their sizing in the AMS (d_{va}), which is not the case in the DMA (d_z). For the equivalent diameters (d_{va} and d_z), the shape of the particle will affect their relationship to d_{ve}. Expressed simply, the mobility diameter increases with increasing deviation from a sphere, while the vacuum aerodynamic diameter decreases as the particles becomes more irregular, i.e. $d_z > d_{ve} > d_{va}$ for irregular particles of standard density.

There are many types of irregular particles in the ambient aerosol. Inorganic salts such as NaCl have crystal-like shapes, soot particles have an agglomerated structure, and fibres and pollen may have varied shapes. The differences in shape can be accounted for by the shape factor or the related volume equivalent diameter, as described briefly above.

Results and Discussion

The short story of soot as CCN

Freshly emitted soot particles do not contribute to the population of CCN (as described in Paper I). Fresh soot agglomerates showed limited hygroscopicity, i.e. they do not become activated and form cloud droplets at supersaturations below 2%. In laboratory measurements on diesel exhaust aerosol, an increase in hygroscopicity was observed immediately (within 5 min) after UV exposure (see Figure 7). This early change in water vapour uptake of the soot particles can probably be attributed to the condensed SOA, formed by intermediate volatility organic compounds in the exhaust. The increase in particle hygroscopicity upon UV exposure indicates that the lifetime of soot particles in the atmosphere is affected by sunlight. As the intensity of sunlight differs with latitude so will the ambient particle lifetime. During the photochemical processing of soot particles, SOA condense onto the soot particles, progressively changing their size and morphology (as can be seen from the TEM images in Figure 7), as well as their chemical composition. Soot particles are thus transformed from a highly agglomerated structure, severely limited hygroscopicity, to compact, almost spherical particles that act as CCN at atmospherically relevant supersaturations (size dependant). The complete transformation in the hygroscopicity of soot particles was captured for the first time in this work, using the SFCA measurement mode in the CCNC (Paper I). The increase in water vapour uptake of the soot particles facilitates the restructuring of the particles, which is visualized by the dip in the diameter measured by the second DMA in the H-TDMA set-up ($d(RH)$, and $gf = d(RH)/d_{dry} < 1$) shown in the inset in Figure 7 and also discussed in Paper IV. Thus, although fresh soot particles contribute to the global warming, after ageing (i.e. the condensation of soluble material onto soot particles) they also act as CCN, leading to cooling.

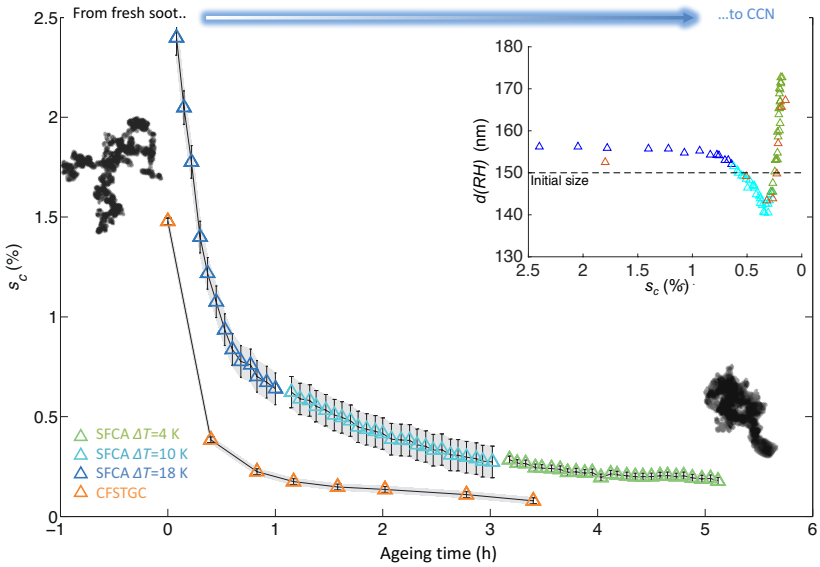

Figure 7. The short story of soot as CCN
The changes in critical supersaturation (s_c) are shown as a function of ageing time (UV exposure) for diesel exhaust particles (soot). At the onset of UV, there was an immediate increase in hygroscopicity, enabling the first measurements on s_c. Results are shown for two different experiments using the traditional CFSTGC measurement mode and the newly implemented SFCA mode at different ΔT. The higher time resolution possible with the latter method is clearly seen. The inset shows the particle mobility diameter measured with the second DMA (*d(RH)*) in the H-TDMA set-up as a function of s_c for the two experiments. An initial particle size of d_z=150 nm (dashed line) was selected in both experiments, and when *d(RH)*<150 nm means that the agglomerates have shrunk due to condensation of the SOA, and that the hygroscopic growth factor is below 1. TEM images of (left) a fresh, highly agglomerated diesel soot particle, and (right) a diesel soot particle that has been restructured into a more spherical shape by ageing are also shown.

Theoretically, the water vapour uptake of the soot particles was predicted using traditional Köhler theory for particles containing more than 80% organic material by mass. However, if the shape of the soot particles was also taken into account, a reliable theoretical prediction of the cloud forming potential, was obtained for soot particles containing only 12% organic material by mass. In the study described in Paper I, it was shown that the volume equivalent diameter was a better measure of the cloud droplet activation, than the mobility diameter when performing calculations with traditional Köhler theory. Also, the volume equivalent diameter was successfully approximated for both diesel soot particles and soot particles from a flame soot generator, using parameterization of d_z and the mass fraction of SOA. The hygroscopicity parameter, κ, was ~0.13 for the anthropogenic SOA produced from the precursors *m*-xylene, toluene and diesel exhaust, and approached 0.13 for the SOA produced from the precursors in the gasoline exhaust (Paper II) with increasing organic coating (i.e. with decreasing influence of the AS seed particles). Hence, the κ value of the laboratory-produced anthropogenic SOA is within the range found in the literature (see examples in Table 1).

Soluble or insoluble – that's the question

Fresh emissions from motor vehicles contain a wide range of compounds in the gaseous and particle phase. The compounds produced and in the phase in which they are formed depend on the combustion conditions and the fuel used. A diesel motor, for example, produces soot particles and gas, while a gasoline motor produces predominantly gases (including SOA precursors). These fresh emissions have a low affinity for water, with hygroscopic growth factors of ~1 at an RH of 90%, and supersaturations of >2% are required (see Figure 7), according to the laboratory measurements performed in this study (Paper I). However, as vehicle emissions are photochemically processed SOA is produced, with a hygroscopicity that increases with ageing. The various anthropogenic particles analysed in this study were: soot particles (from a flame soot generator or a diesel vehicle) coated with SOA produced from precursors in the diesel exhaust and/or toluene and *m*-xylene; and AS particles coated with SOA produced from gasoline vehicles or toluene and *m*-xylene. The anthropogenic SOA was of greatest interest in this work (Paper II). However, the constituents and shape of the primary particles are of importance in understanding the water uptake behaviour.

The water vapour uptake of the anthropogenic SOA produced in this study depends on whether the subsaturation or supersaturation regime is considered, independent of the precursors (Paper II). The water uptake in the subsaturated regime is lower than that in the supersaturated regime. The hygroscopicity parameters derived from the subsaturated (κ_{gf}) and supersaturated (κ_{sc}) regimes differ by up to 72%. To capture this divergent behaviour in water vapour uptake in the two regimes, a modified version of the Köhler theory was used (described in pp.17-21). This modified version takes the limited water solubility of part of the organic material into account. Some of the discrepancy in water vapour uptake (depending on regime) might be attributed to the different measurement techniques used, or to other factors that have been analysed previously, such as a reduction in surface tension and bulk-to-surface partitioning of surface-active compounds (e.g. Hodas et al., 2016; Petters and Kreidenweis, 2013; Ruehl et al., 2010; Wex et al., 2009). In the present work, a reduced surface tension (using constant values between 72 and 30 mN/m) was used in the calculation of the κ values, as a simplified sensitivity test of surface tension effects. The agreement in κ values under the two regimes was improved with reduced surface tension, however, a reduction in surface tension can only partly explain the discrepancy between the κ values from the subsaturated and supersaturated regimes, as was concluded by Wex et al. (2009). A similar study of the effects of surface tension was performed using the modified Köhler theory (based on chemical composition), although no improvement was found in the agreement between the theoretical and the empirical results. Reducing the surface tension reduces the initially good agreement between empirical and theoretical

results, by lowering the theoretical value of s_c, although it had a negligible effect on *gf* predictions, which required improvement for agreement. The discrepancy between the results obtained in the subsaturated and supersaturated regimes is often increased when only the surface tension is reduced, according to McFiggans et al. (2006).

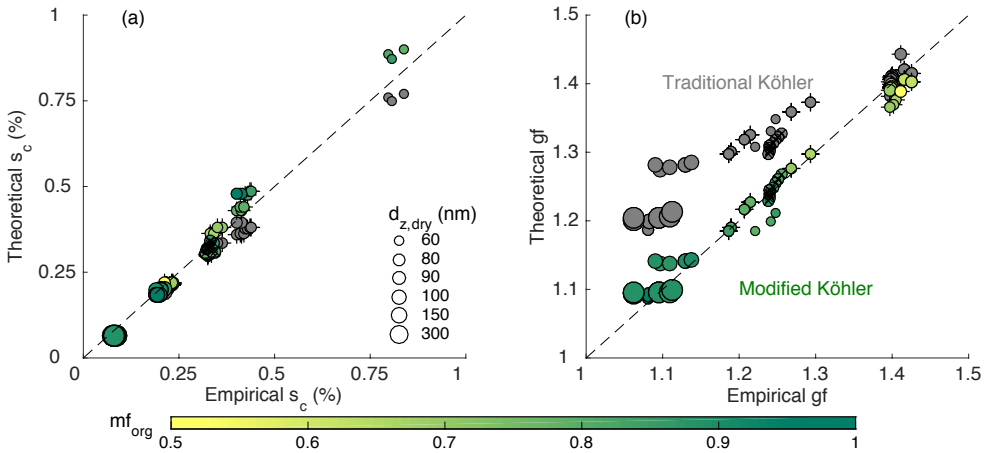

Figure 8. Indications of solubility limitation of the anthropogenic SOA
The theoretical and empirical results show better agreement when the modified Köhler theory is used (green shading), than when using traditional Köhler theory (grey shading). In (a) the critical supersaturation (s_c) shows only minor deviation between the two theoretical approaches, while in (b) the hygroscopic growth factor (*gf*) is much better represented by the modified Köhler theory (where water solubility limitation for part of the organic material is taken into account), than the traditional Köhler theory. Particle diameter, d_z (nm), is indicated by the size of the data points, and the green colour scale indicates the mass fraction of organic material (mf_{org}). The dashed line has a slope of 1. Different types of anthropogenic particles were analysed: soot particles coated with SOA from the precursors in diesel exhaust and/or toluene and *m*-xylene (circles), AS coated with SOA from the precursors in gasoline exhaust (crosses behind the circles) or toluene and *m*-xylene (crosses inside the circles).

The results of this study indicate that limited solubility is responsible for the diverging behaviour in water vapour uptake of the aerosol particles produced from the different anthropogenic emissions, in the two saturation regimes. This means that these particles will affect our climate differently (due to scattering and absorption of light, particle lifetime and scavenging of particles) depending on where in the atmosphere these particles are released and processed. Hypothetically, solubility limitation may delay the activation of atmospheric particles into cloud droplets, or contribute to the formation of large-droplet fog or smog found in heavily polluted regions. Particle water uptake may enhance both the scattering and absorption of light (Khalizov et al., 2009), and thus affect visibility and the climate. In addition, the limitation of water solubility of the particles may have an effect on the particle deposition pattern in human lungs (Londahl et al., 2009) and also affect particle toxicity. However, the effect of the solubility limitation of the organic

material produced from anthropogenic precursors is more important for our understanding of the behaviour of particle water vapour uptake when interpreting laboratory data and particle modelling, than its atmospheric effect.

Urban air pollution – in a hygroscopic perspective

Hygroscopicity measurements were performed during the winter, in the city centre of Copenhagen, Denmark (Paper III). In the subsaturated regime, two main observations were made of the urban aerosol with respect to particle hygroscopicity: (*i*) there is a dependence on air mass origin, and (ii) there is a clear temporal variation. In the literature, a diurnal variation in hygroscopicity as well as the hygroscopicity of urban aerosol particles, are often represented by *gf*'s the lower range. The dependence on air mass origin and also the hygroscopicity of rural aerosol particles are often attributed to particles that have a higher affinity for water (e.g. Laborde et al., 2013; McFiggans et al., 2006). In the present study, the results of external mixture were studied and visualized by particles with a low hygroscopicity in the lower *gf* range (<1.25), i.e. the fraction of the less-hygroscopic particles ($NF_{gf<1.25}$; using H-TDMA), and the number fraction of soot (NF_{soot}; using DMA-APM).

In Figure 9, the dependence on air mass origin is illustrated. In general, the $NF_{gf<1.25}$ of the urban aerosol showed decreasing values with increasing particle size, however, the decrease was not as pronounced when the influencing air was coming from the North Sea (Figure 9a), as from the continent (Figure 9b). The pattern is likely explained by a higher background concentration of hygroscopic particles in the continental air, than in air masses from the North Sea. The influence of air mass origin was confirmed by auxiliary measurements used in the present work; i.e., higher fractions of smaller particles and lower number concentrations is being seen in the urban aerosol when influenced by North Sea air masses (measured with the SMPS), and a clear difference in the chemical composition (measured with the AMS) for the different wind directions. These findings are also in agreement with those made by Rissler et al. (2014), who observed that background particles contributed to the number concentration of fresh soot particles (measured with the DMA-APM set-up, during the same measurement period). Thus, the observations indicate that continental air masses had undergone more atmospheric processing, and as a result included higher number fractions of larger and more hygroscopic particles, than North Sea air masses with larger proportion of local contributions.

The temporal variation of the urban particle hygroscopicity follows the diurnal cycle. This diurnal variation was also confirmed using the other measurement techniques; i.e., higher number fraction of soot during the daytime (NF_{soot}; using DMA-APM), variations in the chemical composition (using AMS and aethalometer), higher number concentration of smaller particles during the daytime

(using SMPS), and variations in the CCN population (using a CCNC). A diurnal variation in CCN has been reported previously (Souto-Oliveira et al., 2016). In this study, it was concluded that a large fraction of the less-hygroscopic particles ($NF_{gf<1.25}$) during the daytime are fresh soot particles produced locally, predominantly by traffic.

The hygroscopicity parameter (κ) derived from the s_c was in the range 0.07-0.21, during one night's measurements in Copenhagen, when the air mass was coming from the North Sea. This range is in agreement with previously reported values for urban aerosol hygroscopicity, as well as laboratory-generated anthropogenic SOA (see Table 1).

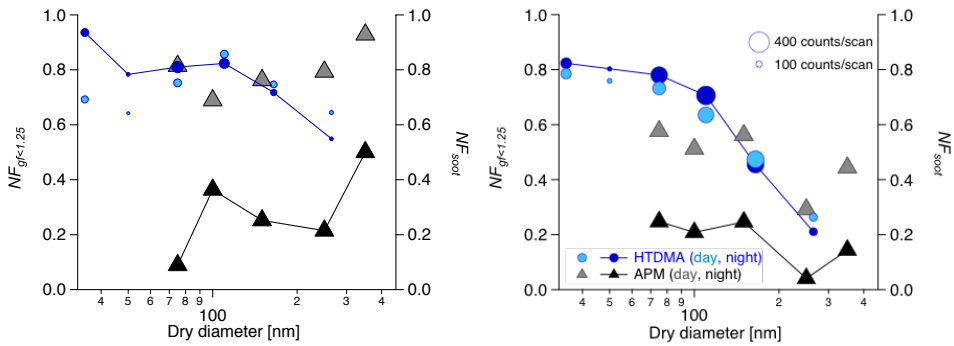

Figure 9. Influence of air masses from the North Sea and continental air masses on urban aerosols
Results from the two instruments (H-TDMA and APM) are compared during which air masses came from (a) the North Sea (for the time period 10.01 12:00 – 14.01 05:00) and (b) the south-east continent (for the time period 25.01 12:00 – 27.01 12:00), and swept over the city. The number fraction of less-hygroscopic particles ($NF_{gf<1.25}$; left axis) as well as the number fraction of soot partilces (NF_{soot}; right axis) as a function of mobility size (d_z in nm). The results are separated into daytime and night-time, and for the H-TDMA the particle counts recorded for each single size measured correspondend proportionally to the number size distribution (measured by the SMPS) at that time. The number of measurements for each data point are between: 71-89 daytime, and 21-41 night-time for the H-TDMA; and 12-24 daytime, and 2-10 night-time for the DMA-APM. It can be seen that urban aerosols influenced by air masses from the North Sea are less-hygroscopic than those influenced by continental air masses (size dependent). During the daytime, the number fraction of less-hygroscopic particles corresponds well with the number fraction of soot, while during the night-time a clear difference was observed.

Figure 9, shows a detailed comparison of $NF_{gf<1.25}$ and NF_{soot}. The urban aerosol was externally mixed, according to results from the H-TDMA and the DMA-APM set-up. The number of particles in the less-hygroscopic fraction shows similar values as in the fraction of soot, during the daytime. However, during the night-time, the $NF_{gf<1.25}$ is larger than the NF_{soot}. A plausible explanation for this is that the soot particles transform due to atmospheric ageing to a more compact and denser form before a pronounced increase in hygroscopicity in the subsaturated regime is seen. This behaviour was observed in the laboratory measurements of this work (illustrated in Paper V).

From urban to rural – Rapid soot transformation

The measurements performed in the urban environment (Copenhagen, Papers III and IV) were combined with observations from a rural measurement station at Vavihill, only 60 km to the northeast of the city, which is part of the European ACTRIS (station network (described in detail by Kristensson et al., 2008), during the winter. The results from measurements of the chemical composition (gases and particles), particle morphology, number concentration and hygroscopicity were evaluated in combination with wind trajectory data (Paper IV), and suggest that the restructuring of ambient soot particles is faster (<5 hours) than previously thought in the dark, cold, and humid conditions of northern Europe. The restructuring of urban soot is due to the fast condensation (one to a few hours) of secondary material (organic and inorganic, especially ammonium nitrate), enabling the particles to take up water, which further facilitates the reshaping of the agglomerates. Thus, understanding the impact of the formation of inorganic secondary material is also very important, in addition to understanding the impact of SOA formation, which is currently the subject of much research in atmospheric science.

Traffic pollution – A perpetrator in a double sense

Traffic emissions make a significant contribution to outdoor air pollution, and are doubly damaging as they contribute to climate change, as well as causing about 4 million premature deaths every year, ~600,000 of which are children under 5 years of age (UNICEF, 2016; WHO, 2016). The effect of traffic pollution will vary and change depending on the retention time in the atmosphere (i.e. the degree of ageing), the composition of the surrounding air (particles and gases that the exhausts are mixed with in the atmosphere), and meteorological conditions (e.g. wind speed, temperature, precipitation). The effect of traffic exhausts on climate is discussed in Paper V, which provides a synthesis in which experimental work together with literature studies are put in perspective.

In this study, it was concluded that freshly emitted soot particles are hydrophobic at atmospherically relevant RH. These fresh soot particles have a highly agglomerated structure, and are known to absorb light, leading to a warming effect (IPCC, 2013). Soot particles and additional gases and particles from the combustion of fossil fuels, are hazardous to human health, particularly to children and elderly people (UNICEF, 2016; WHO, 2016). During atmospheric ageing, soot particles are transformed by condensation of both anthropogenic and biogenic, organic and inorganic compounds. It has been shown that, as the agglomerates are transformed, the absorption of sunlight can be enhanced due to coating of sufficiently transparent materials, which is called the *lensing effect* (e.g. Guo et al., 2016; Peng et al., 2016). The observations in this work (Paper IV) suggest that the transformation of soot agglomerates in the atmosphere is rapid. However, the rate of transformation and

the retention time are highly dependent on the condensing material and the ability of the particle material to take up water vapour. From the laboratory results (Paper II), it was concluded that the hygroscopicity of the SOA material, produced from traffic exhaust, showed limitations in water vapour uptake in the subsaturated regime, but not in the supersaturated regime. This limitation may have implications for the formation of urban smog and fog. After atmospheric ageing for one to a few hours, soot particles contribute to the population of CCN, thus leading to cooling.

The water uptake of the transformed soot particles will affect the particle deposition in the human lungs (Londahl et al., 2009). According to Londahl et al. (2009), the fraction of hydrophobic particles deposited shows a u-shaped pattern, with minimum deposition of particles with a diameter of ~300 nm (d_z). Due to the u-pattern and minimum, the soot particle deposition in the human lung could hypothetically increase, when the soot particles are aged in the atmosphere. Partly aged soot particles restructure into smaller sizes, while fully aged soot particles increase in size due to condensation, both which could lead to an increased deposition. The effects on human health of a change in deposition pattern have not yet been explored. Regardless of whether traffic emissions are fresh or aged, global benefits will be gained by reducing such emissions.

The short time scales for soot transformation, observed in this work together with the observations presented by Peng et al. (2016), have implications on both climate and health. The combined effect of soot particles as a climate forcer may be different from that previously believed. On the one hand, the rapid transformation of soot, from almost hydrophobic to sufficiently hygroscopic to act as CCN, may enhance the role of soot as a climate cooler. On the other hand, the lensing effect might play a larger role during the transformation of soot agglomerates to more spherical shapes, increasing the warming effect of soot. Another effect of rapid transformation might be a shorter lifetime of soot particles, as the wet scavenging can occur faster. Hence, it might be necessary to re-evaluate the extent to which cooling counteracts the warming of our climate by soot particles.

Conclusions and Outlook

The main work in this thesis was to investigate the water vapour uptake of aerosol particles produced from and/or affected by traffic emissions. The work started with the experimental analysis of the hygroscopicity of photochemically processed traffic exhaust, and the coupling of the observations to a theoretical framework (Papers I and II). The complete transformation in hygroscopicity of soot particles – from freshly emitted hydrophobic agglomerates, to highly processed spherical-like soot particles that can act as CCN – was captured for the first time in this work. This was possible due to the implementation of the SFCA measurement mode in the CCNC. A hygroscopicity enhancement in the supersaturated regime and the restructuring of the soot particles were seen long before an increase was visible of the hygroscopicity in the subsaturated regime. It was concluded that the hygroscopicity in the supersaturated regime, of partly aged soot particles (>12% organic material by mass), could be accurately calculated using traditional Köhler theory if the shape of the particle was accounted for. A discrepancy in hygroscopicity, of aged traffic exhaust particles, was observed between measurements made in the subsaturated and the supersaturated regimes. This discrepancy could be accounted for by using a modified version of Köhler theory, taking solubility limitations of the condensing SOA into account.

Hygroscopicity measurements were also performed on ambient urban aerosol particles, showing that there is a diurnal variability, as well as a dependence on air mass origin (Paper III). The number fraction of less-hygroscopic particles was highly correlated to the number fraction of fresh soot (traffic) emissions during the daytime. During the night-time, the fraction of soot decreases, while the hygroscopicity at subsaturation was not notably improved. This behaviour was linked to the observations made during the laboratory measurements presented in this work, and indicates that the soot particles during the night-time were only partly aged. The hygroscopicity parameters derived from critical supersaturation of the laboratory and ambient aerosols produced from traffic exhaust, in this work, are in agreement with the values in the literature. Finally, observations on the transformation of fresh diesel soot particles under cold, dark and humid conditions, indicated that the restructuring and changes in properties may occur much faster (within 5 hours) than previously thought (Paper IV). Coupled particulate nitrate formation and water vapour uptake, play a central role in the transformation process.

The work presented in this thesis is summarized in Paper V, where it is concluded that the effects of fresh and aged traffic exhaust on the Earth's climate are connected to the hygroscopicity of the exhaust particles. The hygroscopicity effect will differ depending on the residence time of the particles in the atmosphere. Fresh soot particles, and those that have been only slightly processed in the atmosphere will lead to warming due to light absorption. However, as condensation of the secondary material continues, the soot particles become part of the CCN population, and can thereby contribute to the cooling of climate by the influencing cloud properties. The condensation of organic material onto the soot particles may enhance particle hygroscopicity, however, not to the same extent as inorganic salts. Thus, condensation of organic and/or inorganic material affect the atmospheric lifetime of aerosol particles, causing further effects on the climate. Changes in the properties of soot due to combustion conditions, the condensation of organic and inorganic material, evaporation, degree of restructuring, environmental conditions, etc., should also be further investigated.

The hygroscopic properties of particles also play a role in deposition in the lungs, and will thus affect human health. Soot has been classified as carcinogenic to humans; however, it is not clear how aged soot particles affect human health. The effect of aged soot particles on human health is clearly a question for future research.

Further development of the scanning flow mode of CCNC analysis is required for future long-term measurements. Better time resolution of the measurements, as well as better coverage of the saturation spectrum for the atmospheric aerosol, could be achieved by further development.

Other, more comprehensive questions must also be addressed, such as how the time scale of soot transformation is related to climate change, and the extent to which aged traffic exhaust affect the climate on both regional and global scales. Particle hygroscopicity probably plays a considerable role in this regard. There is a need for both experimental measurements and modelling efforts, as well as continuous collaboration between fields of atmospheric science, to address these questions.

Acknowledgments

First and foremost, I would like to thank my wonderful supervisor, Senior lecturer Birgitta Svenningsson, for giving me the opportunity to carry out this research. Thank you for giving me this challenge, for your patience, our fruitful discussions, and for sharing your deep knowledge with me.

Secondly, I would like to thank Senior lecturer Jenny Rissler, for being such a good co-supervisor, co-author, co-lleague and friend. You always had interesting ideas and good suggestions, and always had time for me.

I would also like to thank Dr Elisabeth Ahlinder. Without you I would never had considered entering into research at the university. You are a wonderful person, and your friendship is very precious to me.

I would like to express my gratitude to the Swedish Research Council (VR), the Swedish Research Counsil FORMAS, Top-level Research Initiative CRAICC, the Strategic Research Area at Lund University MERGE, and ClimBEco research school for making this research possible.

Thanks also to…

…Senior lecturer Joakim Pagels: I'm happy you took me under your wing and helped me explore the world of traffic exhausts. The content of this thesis would be in a very different shape without you.

…Professor Erik Swietlicki, Dr Erik Fors, and Erik Ahlberg: A great name of great persons. You all contributed valuable ideas, feedback and thoughts, with a big sense of humour – I really appreciate your different levels of input.

…my two comrades in arms, Dr Moa Sporre and Dr Johan Friberg. We set out to save the world, but I don't think we have completed our mission just yet. ;-)

…Dr Staffan Sjögren, your instruction in the laboratory, and help with the implementation of SFCA measurement mode as well as your guidance when evaluating data have been invaluable (not to mention the writing and (weekly) discussions of the Cph manuscript).

…Dr Axel Eriksson, Dr Pontus Roldin, Johan Martinsson, Dr Patrik Nilsson, Ville Malmborg, Senior lecturer Jakob Löndahl, Dr Erik Nordin, Mikael Elfman, and

Robert Olsson: I value your different areas of expertise and help in discussing my ideas and trying them out.

…the staff at the Department of Nuclear Physics, especially Professor Per Kristiansson, Professor Kristina Stenström, Professor Dirk Rudolph, and the head of the Physics Department, Professor Knut Deppert, for being such good bosses.

…Britt-Marie Kallerhed, Anneli Nilsson Ahlm and Yulia Lindholm: for help with all the administrative matters; Charlotta Nilsson for being a great roomate when I started, for simplifying the teaching duties of PhD students, and for keeping track of my many months (85?) of employment; and the Service group for everything concerning my period in the IKDC building.

…everyone I have met in the IKDC building; it was great sharing the lunches, coffee breaks and events with you.

…Maria Messing; for sismance!

…Stefan Olin, my learning partner: we've learned a lot together.

…My mother and father: for everything you've done for me throughout the years.

…Gunnel: tack för all omtanke, ditt stöd och att du ställt upp som barnvakt.

Finally, I owe a huge debt gratitude to my family. My wonderful children: Hilda, Erik and Kajsastina: without you, my period as a PhD student would have gone by too quickly, and been a lot more stressful. Andreas, the love of my life, we did it – at last you have your very own doctor! Hopefully, our late-night scientific and non-scientific discussions (at about 8 pm, before falling asleep), will continue for the rest of our lives…

References

Ackerman, A.S., Toon, O., Stevens, D., Heymsfield, A., Ramanathan, V. and Welton, E., 2000. Reduction of tropical cloudiness by soot. Science, 288(5468): 1042-1047.

ACTRIS, Aerosol, Clouds, Trace gases Infrastructure.

Albrecht, B.A., 1989. Aerosols, cloud microphysics, and fractional cloudiness. Science, 245(4923): 1227-1230.

Andreae, M.O. and Rosenfeld, D., 2008. Aerosol-cloud-precipitation interactions. Part 1. The nature and sources of cloud-active aerosols. Earth-Science Reviews, 89(1-2): 13-41.

Asa-Awuku, A., Engelhart, G.J., Lee, B.H., Pandis, S.N. and Nenes, A., 2009. Relating CCN activity, volatility, and droplet growth kinetics of beta-caryophyllene secondary organic aerosol. Atmospheric Chemistry and Physics, 9(3): 795-812.

Bilde, M. and Svenningsson, B., 2004. CCN activation of slightly soluble organics: the importance of small amounts of inorganic salt and particle phase. Tellus B, 56(2): 128-134.

Bond, T.C., Doherty, S.J., Fahey, D.W., Forster, P.M., Berntsen, T., DeAngelo, B.J., Flanner, M.G., Ghan, S., Karcher, B., Koch, D., Kinne, S., Kondo, Y., Quinn, P.K., Sarofim, M.C., Schultz, M.G., Schulz, M., Venkataraman, C., Zhang, H., Zhang, S., Bellouin, N., Guttikunda, S.K., Hopke, P.K., Jacobson, M.Z., Kaiser, J.W., Klimont, Z., Lohmann, U., Schwarz, J.P., Shindell, D., Storelvmo, T., Warren, S.G. and Zender, C.S., 2013. Bounding the role of black carbon in the climate system: A scientific assessment. Journal of Geophysical Research-Atmospheres, 118(11): 5380-5552.

Brimblecombe, P., 1978. Air-Pollution in Industrializing England. Journal of the Air Pollution Control Association, 28(2): 115-118.

Broekhuizen, K., Kumar, P.P. and Abbatt, J.P.D., 2004. Partially soluble organics as cloud condensation nuclei: Role of trace soluble and surface active species. Geophysical Research Letters, 31(1).

Carlton, A.G., Pinder, R.W., Bhave, P.V. and Pouliot, G.A., 2010. To What Extent Can Biogenic SOA be Controlled? Environmental Science & Technology, 44(9): 3376-3380.

Chang, R.Y.W., Slowik, J.G., Shantz, N.C., Vlasenko, A., Liggio, J., Sjostedt, S.J., Leaitch, W.R. and Abbatt, J.P.D., 2010. The hygroscopicity parameter (kappa) of ambient organic aerosol at a field site subject to biogenic and anthropogenic influences: relationship to degree of aerosol oxidation. Atmospheric Chemistry and Physics, 10(11): 5047-5064.

Covert, D.S., Wiedensohler, A., Aalto, P., Heintzenberg, J., McMurry, P.H. and Leck, C., 1996. Aerosol number size distributions from 3 to 500 nm diameter in the arctic marine boundary layer during summer and autumn. Tellus Series B-Chemical and Physical Meteorology, 48(2): 197-212.

DeCarlo, P.F., Kimmel, J.R., Trimborn, A., Northway, M.J., Jayne, J.T., Aiken, A.C., Gonin, M., Fuhrer, K., Horvath, T. and Docherty, K.S., 2006. Field-deployable, high-resolution, time-of-flight aerosol mass spectrometer. Analytical Chemistry, 78(24): 8281-8289.

DeCarlo, P.F., Slowik, J.G., Worsnop, D.R., Davidovits, P. and Jimenez, J.L., 2004. Particle morphology and density characterization by combined mobility and aerodynamic diameter measurements. Part 1: Theory. Aerosol Science and Technology, 38(12): 1185-1205.

Drinovec, L., Mocnik, G., Zotter, P., Prevot, A.S.H., Ruckstuhl, C., Coz, E., Rupakheti, M., Sciare, J., Muller, T., Wiedensohler, A. and Hansen, A.D.A., 2015. The "dual-spot" Aethalometer: an improved measurement of aerosol black carbon with real-time loading compensation. Atmospheric Measurement Techniques, 8(5): 1965-1979.

Duplissy, J., Gysel, M., Alfarra, M.R., Dommen, J., Metzger, A., Prevot, A.S.H., Weingartner, E., Laaksonen, A., Raatikainen, T., Good, N., Turner, S.F., McFiggans, G. and Baltensperger, U., 2008. Cloud forming potential of secondary organic aerosol under near atmospheric conditions. Geophysical Research Letters, 35(3).

Fors, E.O., Rissler, J., Massling, A., Svenningsson, B., Andreae, M.O., Dusek, U., Frank, G.P., Hoffer, A., Bilde, M., Kiss, G., Janitsek, S., Henning, S., Facchini, M.C., Decesari, S. and Swietlicki, E., 2010. Hygroscopic properties of Amazonian biomass burning and European background HULIS and investigation of their effects on surface tension with two models linking H-TDMA to CCNC data. Atmospheric Chemistry and Physics, 10(12): 5625-5639.

Fors, E.O., Swietlicki, E., Svenningsson, B., Kristensson, A., Frank, G.P. and Sporre, M., 2011. Hygroscopic properties of the ambient aerosol in southern Sweden - a two year study. Atmospheric Chemistry and Physics, 11(16): 8343-8361.

Frosch, M., Bilde, M., Nenes, A., Praplan, A.P., Jurányi, Z., Dommen, J., Gysel, M., Weingartner, E. and Baltensperger, U., 2013. CCN activity and volatility of β-caryophyllene secondary organic aerosol. Atmospheric Chemistry and Physics, 13(4): 2283-2297.

Gunthe, S.S., King, S.M., Rose, D., Chen, Q., Roldin, P., Farmer, D.K., Jimenez, J.L., Artaxo, P., Andreae, M.O., Martin, S.T. and Poschl, U., 2009. Cloud condensation nuclei in pristine tropical rainforest air of Amazonia: size-resolved measurements and modeling of atmospheric aerosol composition and CCN activity. Atmospheric Chemistry and Physics, 9(19): 7551-7575.

Guo, S., Hu, M., Lin, Y., Gomez-Hernandez, M., Zamora, M.L., Peng, J.F., Collins, D.R. and Zhang, R.Y., 2016. OH-Initiated Oxidation of m-Xylene on Black Carbon Aging. Environmental Science & Technology, 50(16): 8605-8612.

Gysel, M., McFiggans, G.B. and Coe, H., 2009. Inversion of tandem differential mobility analyser (TDMA) measurements. Journal of Aerosol Science, 40(2): 134-151.

Gysel, M., Nyeki, S., Weingartner, E., Baltensperger, U., Giebl, H., Hitzenberger, R., Petzold, A. and Wilson, C.W., 2003. Properties of jet engine combustion particles during the PartEmis experiment: Hygroscopicity at subsaturated conditions. Geophysical Research Letters, 30(11).

Hinds, W.C., 2012. Aerosol technology: properties, behavior, and measurement of airborne particles. John Wiley & Sons.

Hodas, N., Zuend, A., Schilling, K., Berkemeier, T., Shiraiwa, M., Flagan, R.C. and Seinfeld, J.H., 2016. Discontinuities in hygroscopic growth below and above water saturation for laboratory surrogates of oligomers in organic atmospheric aerosols. Atmospheric Chemistry and Physics, 16(19): 12767-12792.

Hoyle, C.R., Boy, M., Donahue, N.M., Fry, J.L., Glasius, M., Guenther, A., Hallar, A.G., Hartz, K.H., Petters, M.D., Petaja, T., Rosenoern, T. and Sullivan, A.P., 2011. A review of the anthropogenic influence on biogenic secondary organic aerosol. Atmospheric Chemistry and Physics, 11(1): 321-343.

Huff Hartz, K.E., Rosenørn, T., Ferchak, S.R., Raymond, T.M., Bilde, M., Donahue, N.M. and Pandis, S.N., 2005. Cloud condensation nuclei activation of monoterpene and sesquiterpene secondary organic aerosol. Journal of Geophysical Research: Atmospheres (1984–2012), 110(D14).

IPCC, 2013. IPCC 2013: "Climate Change 2013: The Physical Science Basis. Working Group I Contribution to the IPCC 5th Assessment Report - Changes to the Underlying Scientific/Technical Assessment" (IPCC-XXVI/Doc.4). .

IPCC, 2014. Climate Change 2014: Synthesis Report. Contribution of Working Groups I, II, and III to the Fifth Assessment Report of the Intergovernmental Panel on Climate Change Geneva, Switzerland.

Jimenez, J.L., Canagaratna, M.R., Donahue, N.M., Prevot, A.S.H., Zhang, Q., Kroll, J.H., DeCarlo, P.F., Allan, J.D., Coe, H., Ng, N.L., Aiken, A.C., Docherty, K.S., Ulbrich, I.M., Grieshop, A.P., Robinson, A.L., Duplissy, J., Smith, J.D., Wilson, K.R., Lanz, V.A., Hueglin, C., Sun, Y.L., Tian, J., Laaksonen, A., Raatikainen, T., Rautiainen, J., Vaattovaara, P., Ehn, M., Kulmala, M., Tomlinson, J.M., Collins, D.R., Cubison, M.J., Dunlea, E.J., Huffman, J.A., Onasch, T.B., Alfarra, M.R., Williams, P.I., Bower, K., Kondo, Y., Schneider, J., Drewnick, F., Borrmann, S., Weimer, S., Demerjian, K., Salcedo, D., Cottrell, L., Griffin, R., Takami, A., Miyoshi, T., Hatakeyama, S., Shimono, A., Sun, J.Y., Zhang, Y.M., Dzepina, K., Kimmel, J.R., Sueper, D., Jayne, J.T., Herndon, S.C., Trimborn, A.M., Williams, L.R., Wood, E.C., Middlebrook, A.M., Kolb, C.E., Baltensperger, U. and Worsnop, D.R., 2009. Evolution of Organic Aerosols in the Atmosphere. Science, 326(5959): 1525-1529.

Juranyi, Z., Tritscher, T., Gysel, M., Laborde, M., Gomes, L., Roberts, G., Baltensperger, U. and Weingartner, E., 2013. Hygroscopic mixing state of urban aerosol derived from size-resolved cloud condensation nuclei measurements during the MEGAPOLI campaign in Paris. Atmospheric Chemistry and Physics, 13(13): 6431-6446.

Kanakidou, M., Seinfeld, J.H., Pandis, S.N., Barnes, I., Dentener, F.J., Facchini, M.C., Van Dingenen, R., Ervens, B., Nenes, A., Nielsen, C.J., Swietlicki, E., Putaud, J.P., Balkanski, Y., Fuzzi, S., Horth, J., Moortgat, G.K., Winterhalter, R., Myhre, C.E.L., Tsigaridis, K., Vignati, E., Stephanou, E.G. and Wilson, J., 2005. Organic aerosol

and global climate modelling: a review. Atmospheric Chemistry and Physics, 5: 1053-1123.

Khalizov, A.F., Xue, H.X., Wang, L., Zheng, J. and Zhang, R.Y., 2009. Enhanced Light Absorption and Scattering by Carbon Soot Aerosol Internally Mixed with Sulfuric Acid. Journal of Physical Chemistry A, 113(6): 1066-1074.

Kristensson, A., Dal Maso, M., Swietlicki, E., Hussein, T., Zhou, J., Kerminen, V.M. and Kulmala, M., 2008. Characterization of new particle formation events at a background site in Southern Sweden: relation to air mass history. Tellus Series B-Chemical and Physical Meteorology, 60(3): 330-344.

Kulmala, M., Laaksonen, A., Charlson, R.J. and Korhonen, P., 1997. Clouds without supersaturation. Nature, 388(6640): 336-337.

Kuwata, M., Shao, W., Lebouteiller, R. and Martin, S.T., 2013. Classifying organic materials by oxygen-to-carbon elemental ratio to predict the activation regime of Cloud Condensation Nuclei (CCN). Atmospheric Chemistry and Physics, 13(10): 5309-5324.

Laborde, M., Crippa, M., Tritscher, T., Juranyi, Z., Decarlo, P.F., Temime-Roussel, B., Marchand, N., Eckhardt, S., Stohl, A., Baltensperger, U., Prevot, A.S.H., Weingartner, E. and Gysel, M., 2013. Black carbon physical properties and mixing state in the European megacity Paris. Atmospheric Chemistry and Physics, 13(11): 5831-5856.

Lamb, D. and Verlinde, J., 2011. Physics and chemistry of clouds. Cambridge University Press.

Lambe, A.T., Onasch, T.B., Massoli, P., Croasdale, D.R., Wright, J.P., Ahern, A.T., Williams, L.R., Worsnop, D.R., Brune, W.H. and Davidovits, P., 2011. Laboratory studies of the chemical composition and cloud condensation nuclei (CCN) activity of secondary organic aerosol (SOA) and oxidized primary organic aerosol (OPOA). Atmospheric Chemistry and Physics, 11(17): 8913-8928.

Lance, S., Medina, J., Smith, J.N. and Nenes, A., 2006. Mapping the operation of the DMT Continuous Flow CCN counter. Aerosol Science and Technology, 40(4): 242-254.

Lide, D.R., 2005. CRC Handbook of Chemistry and Physics, Internet Version. CRC Press, Boca Raton, FL.

Londahl, J., Massling, A., Swietlicki, E., Brauner, E.V., Ketzel, M., Pagels, J. and Loft, S., 2009. Experimentally Determined Human Respiratory Tract Deposition of Airborne Particles at a Busy Street. Environmental Science & Technology, 43(13): 4659-4664.

Löndahl, J., Pagels, J., Boman, C., Swietlicki, E., Massling, A., Rissler, J., Blomberg, A., Bohgard, M. and Sandström, T., 2008. Deposition of biomass combustion aerosol particles in the human respiratory tract. Inhalation toxicology, 20(10): 923-933.

Ma, X., Zangmeister, C.D., Gigault, J., Mulholland, G.W. and Zachariah, M.R., 2013. Soot aggregate restructuring during water processing. Journal of Aerosol Science, 66: 209-219.

Martin, M., Tritscher, T., Juranyi, Z., Heringa, M.F., Sierau, B., Weingartner, E., Chirico, R., Gysel, M., Prevot, A.S.H., Baltensperger, U. and Lohmann, U., 2013. Hygroscopic properties of fresh and aged wood burning particles. Journal of Aerosol Science, 56: 15-29.

McFiggans, G., Artaxo, P., Baltensperger, U., Coe, H., Facchini, M.C., Feingold, G., Fuzzi, S., Gysel, M., Laaksonen, A., Lohmann, U., Mentel, T.F., Murphy, D.M., O'Dowd, C.D., Snider, J.R. and Weingartner, E., 2006. The effect of physical and chemical aerosol properties on warm cloud droplet activation. Atmospheric Chemistry and Physics, 6: 2593-2649.

McGrath, M., 2016. Four major cities move to ban diesel vehicles by 2025. BBC News, Science and Environment.

McMurry, P.H., Wang, X., Park, K. and Ehara, K., 2002. The relationship between mass and mobility for atmospheric particles: A new technique for measuring particle density. Aerosol Science and Technology, 36(2): 227-238.

Moore, R.H. and Nenes, A., 2009. Scanning Flow CCN Analysis—A Method for Fast Measurements of CCN Spectra. Aerosol Science and Technology, 43(12): 1192-1207.

Nilsson, E., Swietlicki, E., Sjogren, S., Löndahl, J., Nyman, M. and Svenningsson, B., 2009. Development of an H-TDMA for long-term unattended measurement of the hygroscopic properties of atmospheric aerosol particles. Atmospheric Measurement Techniques, 2(1): 313-318.

Novakov, T. and Rosen, H., 2013. The Black Carbon Story: Early History and New Perspectives. Ambio, 42(7): 840-851.

Onasch, T., Trimborn, A., Fortner, E., Jayne, J., Kok, G., Williams, L., Davidovits, P. and Worsnop, D., 2012. Soot particle aerosol mass spectrometer: development, validation, and initial application. Aerosol Science and Technology, 46(7): 804-817.

Pagels, J., Khalizov, A.F., McMurry, P.H. and Zhang, R.Y., 2009. Processing of Soot by Controlled Sulphuric Acid and Water CondensationMass and Mobility Relationship. Aerosol Science and Technology, 43(7): 629-640.

Peng, J.F., Hu, M., Guo, S., Du, Z.F., Zheng, J., Shang, D.J., Zamora, M.L., Zeng, L.M., Shao, M., Wu, Y.S., Zheng, J., Wang, Y., Glen, C.R., Collins, D.R., Molina, M.J. and Zhang, R.Y., 2016. Markedly enhanced absorption and direct radiative forcing of black carbon under polluted urban environments. Proceedings of the National Academy of Sciences of the United States of America, 113(16): 4266-4271.

Petters, M. and Kreidenweis, S., 2007. A single parameter representation of hygroscopic growth and cloud condensation nucleus activity. Atmospheric Chemistry and Physics, 7(8): 1961-1971.

Petters, M.D. and Kreidenweis, S.M., 2013. A single parameter representation of hygroscopic growth and cloud condensation nucleus activity - Part 3: Including surfactant partitioning. Atmospheric Chemistry and Physics, 13(2): 1081-1091.

Petters, M.D., Wex, H., Carrico, C.M., Hallbauer, E., Massling, A., McMeeking, G.R., Poulain, L., Wu, Z., Kreidenweis, S.M. and Stratmann, F., 2009. Towards closing the gap between hygroscopic growth and activation for secondary organic aerosol - Part 2: Theoretical approaches. Atmospheric Chemistry and Physics, 9(12): 3999-4009.

Petzold, A., Ogren, J.A., Fiebig, M., Laj, P., Li, S.M., Baltensperger, U., Holzer-Popp, T., Kinne, S., Pappalardo, G., Sugimoto, N., Wehrli, C., Wiedensohler, A. and Zhang, X.Y., 2013. Recommendations for reporting "black carbon" measurements. Atmospheric Chemistry and Physics, 13(16): 8365-8379.

Pincus, R. and Baker, M.B., 1994. Effect of precipitation on the albedo susceptibility of clouds in the marine boundary layer. Nature, 372(6503): 250-252.

Poschl, U., Rose, D. and Andreae, M.O., 2009. Part 2: Particle Hygroscopicity and Cloud Condensation Nucleus Activity. Clouds in the Perturbed Climate System: Their Relationship to Energy Balance, Atmospheric Dynamics, and Precipitation: 58-72.

Prenni, A.J., Petters, M.D., Kreidenweis, S.M., DeMott, P.J. and Ziemann, P.J., 2007. Cloud droplet activation of secondary organic aerosol. Journal of Geophysical Research-Atmospheres, 112(D10).

Pruppacher, H.R. and Klett, J.D., 1997. Microphysics of Clouds and Precipitation. Kluwer Academic Puplishers, Dordrecht, Netherlands, 954 pp.

Raymond, T.M. and Pandis, S.N., 2002. Cloud activation of single-component organic aerosol particles. Journal of Geophysical Research: Atmospheres, 107(D24): AAC 16-1-AAC 16-8.

Rissler, J., Messing, M.E., Malik, A.I., Nilsson, P.T., Nordin, E.Z., Bohgard, M., Sanati, M. and Pagels, J.H., 2013. Effective Density Characterization of Soot Agglomerates from Various Sources and Comparison to Aggregation Theory. Aerosol Science and Technology, 47(7): 792-805.

Rissler, J., Nordin, E.Z., Eriksson, A.C., Nilsson, P.T., Frosch, M., Sporre, M.K., Wierzbicka, A., Svenningsson, B., Londahl, J., Messing, M.E., Sjogren, S., Hemmingsen, J.G., Loft, S., Pagels, J.H. and Swietlicki, E., 2014. Effective Density and Mixing State of Aerosol Particles in a Near-Traffic Urban Environment. Environmental Science & Technology, 48(11): 6300-6308.

Rissler, J., Svenningsson, B., Fors, E.O., Bilde, M. and Swietlicki, E., 2010. An evaluation and comparison of cloud condensation nucleus activity models: Predicting particle critical saturation from growth at subsaturation. Journal of Geophysical Research, 115(D22).

Rissler, J., Swietlicki, E., Bengtsson, A., Boman, C., Pagels, J., Sandstrom, T., Blomberg, A. and Londahl, J., 2012. Experimental determination of deposition of diesel exhaust particles in the human respiratory tract. Journal of Aerosol Science, 48: 18-33.

Rissler, J., Vestin, A., Swietlicki, E., Fisch, G., Zhou, J., Artaxo, P. and Andreae, M.O., 2006. Size distribution and hygroscopic properties of aerosol particles from dry-season biomass burning in Amazonia. Atmospheric Chemistry and Physics, 6: 471-491.

Roberts, G.C. and Nenes, A., 2005. A Continuous-Flow Streamwise Thermal-Gradient CCN Chamber for Atmospheric Measurements. Aerosol Science and Technology, 39(3): 206-221.

Rodhe, H., 1992. Time scales characterizing the processing of water and cloud condensation nuclei by clouds. CM-80, International Meteorological Institue in Stockholm, Department of Meteorology Stockholm University.

Rose, D., Gunthe, S. S., Mikhailov, E., Frank, G. P., Dusek, U., Andreae, M. O., and Pöschl, U., 2008. Calibration and measurement uncertainties of a continuous-flow cloud condensation nuclei counter (DMT-CCNC): CCN activation of ammonium sulfate and sodium chloride aerosol particles in theory and experiment. Atmos. Chem. Phys.(8): 1153–1179.

Rose, D., Nowak, A., Achtert, P., Wiedensohler, A., Hu, M., Shao, M., Zhang, Y., Andreae, M.O. and Poschl, U., 2010. Cloud condensation nuclei in polluted air and biomass burning smoke near the mega-city Guangzhou, China - Part 1: Size-resolved measurements and implications for the modeling of aerosol particle hygroscopicity and CCN activity. Atmospheric Chemistry and Physics, 10(7): 3365-3383.

Rose, D., Wehner, B., Ketzel, M., Engler, C., Voigtländer, J., Tuch, T. and Wiedensohler, A., 2006. Atmospheric number size distributions of soot particles and estimation of emission factors. Atmospheric Chemistry and Physics, 6(4): 1021-1031.

Rosenørn, T., Kiss, G. and Bilde, M., 2006. Cloud droplet activation of saccharides and levoglucosan particles. Atmospheric Environment, 40(10): 1794-1802.

Ruehl, C.R., Chuang, P.Y. and Nenes, A., 2010. Aerosol hygroscopicity at high (99 to 100%) relative humidities. Atmospheric Chemistry and Physics, 10(3): 1329-1344.

Schnitzler, E.G., Dutt, A., Charbonneau, A.M., Olfert, J.S. and Jager, W., 2014. Soot Aggregate Restructuring Due to Coatings of Secondary Organic Aerosol Derived from Aromatic Precursors. Environmental Science & Technology, 48(24): 14309-14316.

Seinfeld, J.H. and Pandis, S.N., 2006. Atmospheric Chemistry and Physics. John Wiley & Sons Hoboken, New Jersey, 1203 pp.

Shi, J.P., Khan, A.A. and Harrison, R.M., 1999. Measurements of ultrafine particle concentration and size distribution in the urban atmosphere. Science of the Total Environment, 235(1-3): 51-64.

Shilling, J.E., Zaveri, R.A., Fast, J.D., Kleinman, L., Alexander, M.L., Canagaratna, M.R., Fortner, E., Hubbe, J.M., Jayne, J.T., Sedlacek, A., Setyan, A., Springston, S., Worsnop, D.R. and Zhang, Q., 2013. Enhanced SOA formation from mixed anthropogenic and biogenic emissions during the CARES campaign. Atmospheric Chemistry and Physics, 13(4): 2091-2113.

Shinozuka, Y., Clarke, A.D., DeCarlo, P.F., Jimenez, J.L., Dunlea, E.J., Roberts, G.C., Tomlinson, J.M., Collins, D.R., Howell, S.G., Kapustin, V.N., McNaughton, C.S. and Zhou, J., 2009. Aerosol optical properties relevant to regional remote sensing of CCN activity and links to their organic mass fraction: airborne observations over Central Mexico and the US West Coast during MILAGRO/INTEX-B. Atmospheric Chemistry and Physics, 9(18): 6727-6742.

Shulman, M.L., Jacobson, M.C., Charlson, R.J., Synovec, R.E. and Young, T.E., 1996. Dissolution behavior and surface tension effects of organic compounds in nucleating cloud droplets (vol 23, pg 277, 1996). Geophysical Research Letters, 23(5): 603-603.

Souto-Oliveira, C.E., Andrade, M.D.F., Kumar, P., Lopes, F.J.D.S., Babinski, M. and Landulfo, E., 2016. Effect of vehicular traffic, remote sources and new particle formation on the activation properties of cloud condensation nuclei in the megacity of São Paulo, Brazil. Atmos. Chem. Phys., 16(22): 14635-14656.

Spracklen, D.V., Jimenez, J.L., Carslaw, K.S., Worsnop, D.R., Evans, M.J., Mann, G.W., Zhang, Q., Canagaratna, M.R., Allan, J., Coe, H., McFiggans, G., Rap, A. and Forster, P., 2011. Aerosol mass spectrometer constraint on the global secondary organic aerosol budget. Atmospheric Chemistry and Physics, 11(23): 12109-12136.

Svenningsson, B. and Bilde, M., 2008. Relaxed step functions for evaluation of CCN counter data on size-separated aerosol particles. Journal of Aerosol Science, 39(7): 592-608.

Thomas, M.D., 1952. The present status of the development of instrumentation from the study of air pollution, Proceedings National Air Pollution Symposium, pp. 16-23.

Tree, D.R. and Svensson, K.I., 2007. Soot processes in compression ignition engines. Progress in Energy and Combustion Science, 33(3): 272-309.

Tritscher, T., Jurányi, Z., Martin, M., Chirico, R., Gysel, M., Heringa, M.F., DeCarlo, P.F., Sierau, B., Prévôt, A.S.H., Weingartner, E. and Baltensperger, U., 2011. Changes of hygroscopicity and morphology during ageing of diesel soot. Environmental Research Letters, 6(3): 034026.

Twomey, S., 1974. Pollution and the planetary albedo. Atmospheric Environment (1967), 8(12): 1251-1256.

UNHCR, 2015. UNHCR, the Environment and Climate Change, Geneva, Switzerland.

UNICEF, 2016. Clear air for children. 978-92-806-4854-6

Vermeulen, R., Silverman, D.T., Garshick, E., Vlaanderen, J., Portengen, L. and Steenland, K., 2014. Exposure-Response Estimates for Diesel Engine Exhaust and Lung Cancer Mortality Based on Data from Three Occupational Cohorts. Environmental Health Perspectives, 122(2): 172-177.

Weber, S., Kuttler, W. and Weber, K., 2006. Flow characteristics and particle mass and number concentration variability within a busy urban street canyon. Atmospheric Environment, 40(39): 7565-7578.

Wehner, B. and Wiedensohler, A., 2003. Long term measurements of submicrometer urban aerosols: statistical analysis for correlations with meteorological conditions and trace gases. Atmospheric Chemistry and Physics, 3: 867-879.

Weingartner, E., Burtscher, H. and Baltensperger, U., 1997. Hygroscopic properties of carbon and diesel soot particles. Atmospheric Environment, 31(15): 2311-2327.

Wex, H., Petters, M.D., Carrico, C.M., Hallbauer, E., Massling, A., McMeeking, G.R., Poulain, L., Wu, Z., Kreidenweis, S.M. and Stratmann, F., 2009. Towards closing the gap between hygroscopic growth and activation for secondary organic aerosol: Part 1-Evidence from measurements. Atmospheric Chemistry and Physics, 9(12): 3987-3997.

WHO, 2012. Public health round-up: Diesel exhaust carcinogenic, Bulletin of the World Health Organization.

WHO, 2014. 7 million premature deaths annually linked to air pollution. World Health Organization, Geneva.

WHO, 2016. Climate change and health, Media Centre, Fact Sheet.

Wilkins, E., 1954. Air pollution and the London fog of December, 1952. Journal of the Royal Sanitary Institute, 74(1): 1-15.

Wittbom, C., 2014. Cloud Droplet Forming Potential of Ageing Soot and Surfactant Particles - Laboratory research and Köhler modelling, Lund University, Lund, 35 pp.

Wu, Z.J., Poulain, L., Henning, S., Dieckmann, K., Birmili, W., Merkel, M., van Pinxteren, D., Spindler, G., Muller, K., Stratmann, F., Herrmann, H. and

Wiedensohler, A., 2013. Relating particle hygroscopicity and CCN activity to chemical composition during the HCCT-2010 field campaign. Atmospheric Chemistry and Physics, 13(16): 7983-7996.

Zhang, R.Y., Khalizov, A.F., Pagels, J., Zhang, D., Xue, H.X. and McMurry, P.H., 2008. Variability in morphology, hygroscopicity, and optical properties of soot aerosols during atmospheric processing. Proceedings of the National Academy of Sciences of the United States of America, 105(30): 10291-10296.

Zhao, D.F., Buchholz, A., Kortner, B., Schlag, P., Rubach, F., Fuchs, H., Kiendler-Scharr, A., Tillmann, R., Wahner, A., Watne, Å.K., Hallquist, M., Flores, J.M., Rudich, Y., Kristensen, K., Hansen, A.M.K., Glasius, M., Kourtchev, I., Kalberer, M. and Mentel, T.F., 2016. Cloud condensation nuclei activity, droplet growth kinetics, and hygroscopicity of biogenic and anthropogenic secondary organic aerosol (SOA). Atmos. Chem. Phys., 16(2): 1105-1121.

Zhao, D.F., Buchholz, A., Kortner, B., Schlag, P., Rubach, F., Kiendler-Scharr, A., Tillmann, R., Wahner, A., Flores, J.M., Rudich, Y., Watne, Å.K., Hallquist, M., Wildt, J. and Mentel, T.F., 2015. Size-dependent hygroscopicity parameter (κ) and chemical composition of secondary organic cloud condensation nuclei. Geophysical Research Letters, 42(24): 10,920-10,928.

Zuberi, B., Johnson, K.S., Aleks, G.K., Molina, L.T. and Laskin, A., 2005. Hydrophilic properties of aged soot. Geophysical Research Letters, 32(1).

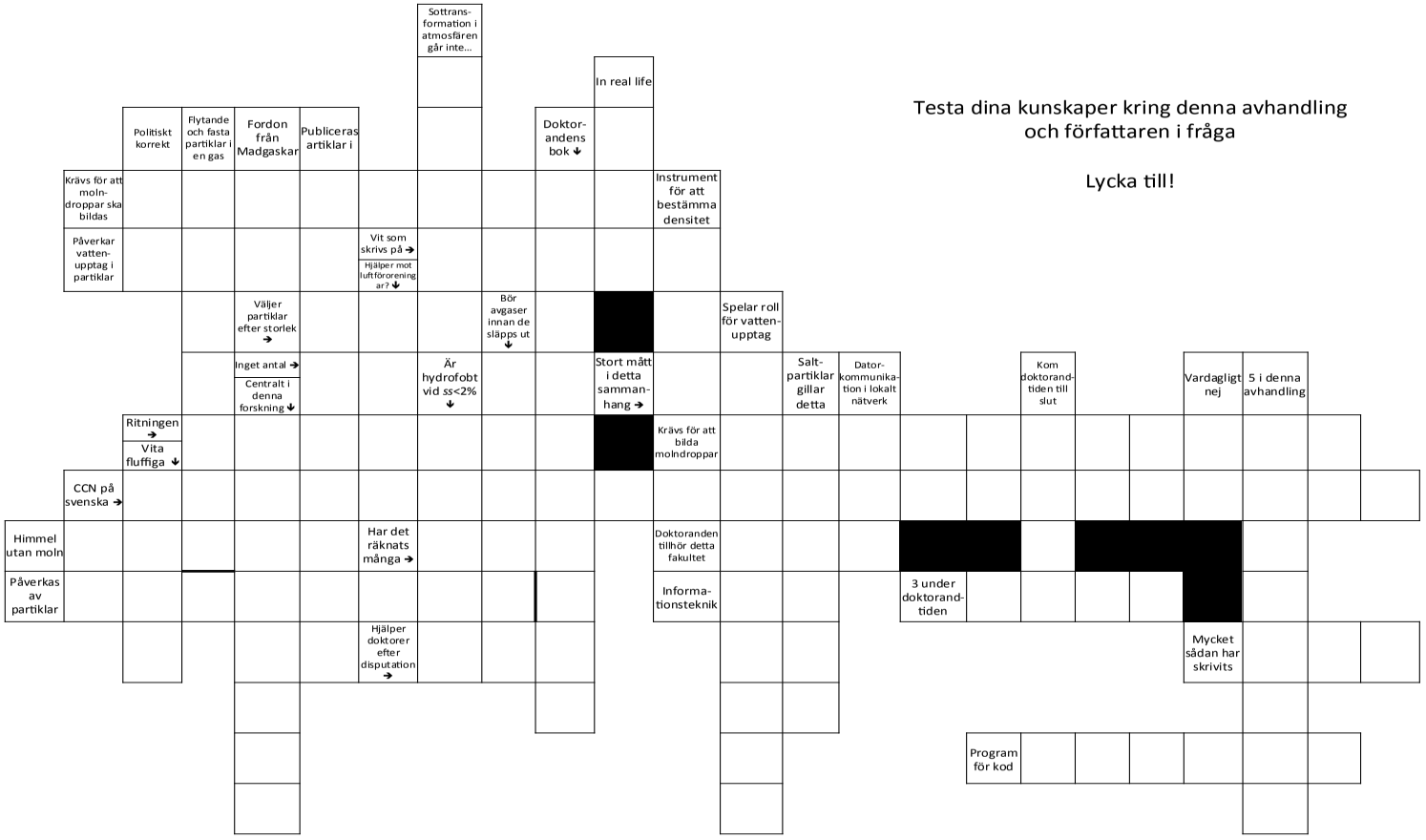
Testa dina kunskaper kring denna avhandling och författaren i fråga
Lycka till!
Sottrans-formation i atmosfären går inte...
In real life
Politiskt korrekt
Flytande och fasta partiklar i en gas
Fordon från Madgaskar
Publiceras artiklar i
Doktor-andens bok
Krävs för att moln-droppar ska bildas
Instrument för att bestämma densitet
Påverkar vatten-upptag i partiklar
Vit som skrivs på
Hjälper mot luftförorening ar?
Väljer partiklar efter storlek
Bör avgaser innan de släpps ut
Spelar roll för vatten-upptag
Inget antal
Centralt i denna forskning
Är hydrofobt vid ss<2%
Stort mått i detta samman-hang
Salt-partiklar gillar detta
Dator-kommunika-tion i lokalt nätverk
Kom doktorand-tiden till slut
Vardagligt nej
5 i denna avhandling
Ritningen
Vita fluffiga
Krävs för att bilda molndroppar
CCN på svenska
Himmel utan moln
Har det räknats många
Doktoranden tillhör detta fakultet
Påverkas av partiklar
Informa-tionsteknik
3 under doktorand-tiden
Hjälper doktorer efter disputation
Mycket sådan har skrivits
Program för kod